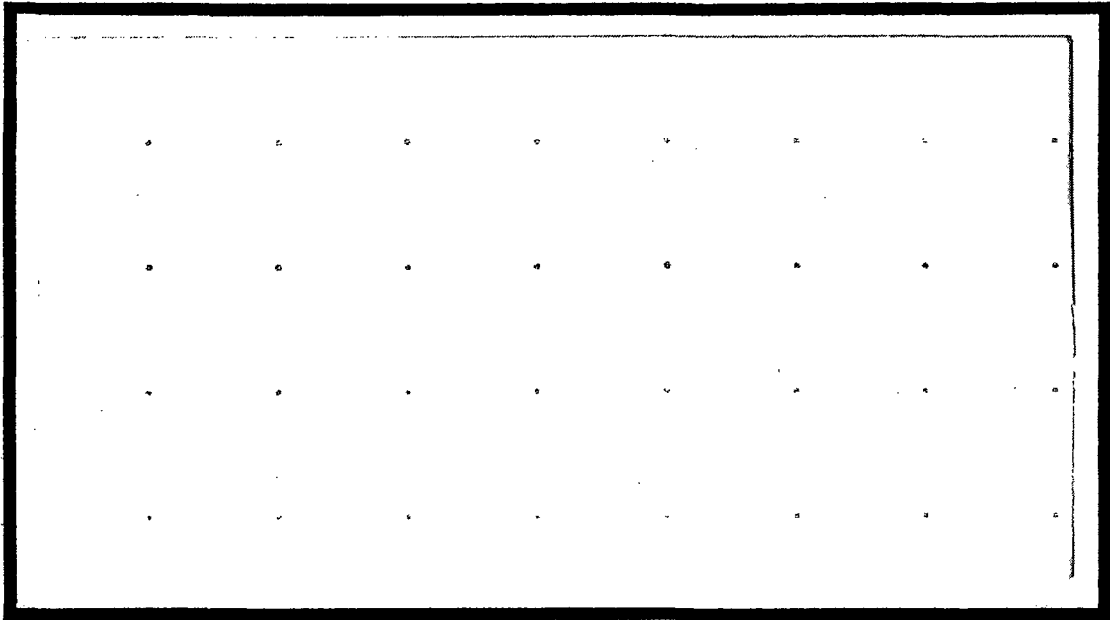
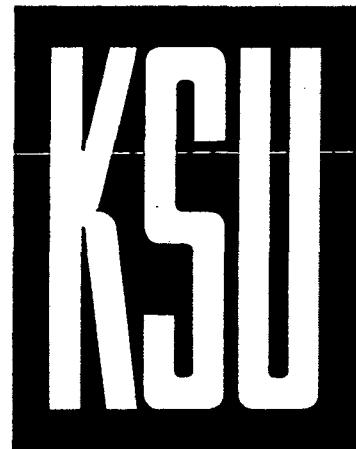


N 7 2 - 2 8 8 2 0



**CASE FILE
COPY**



KANSAS STATE UNIVERSITY • MANHATTAN, KANSAS

SEMI-ANNUAL STATUS REPORT

Infrared Laboratory Studies of
Synthetic Planetary Atmospheres

Grant NGR 17-001-026

This report covers work for the period

1 December 1971 to 31 May 1972

It was prepared by

Prof. Dudley Williams, Department of Physics

Kansas State University, Manhattan, Kansas

Date: 20 June 1972

I. ABSTRACT OF RESEARCH TO DATE

The general program represents an extension and generalization of an earlier program dealing chiefly with telluric gases. The basic instrumentation includes three Perkin-Elmer Model 112 spectrometers equipped with prisms to cover the range between the visible and 40 microns, one Perkin-Elmer Model 421 grating instrument for the 2- to 18 micron region, and a Perkin-Elmer Model 301 far-infrared spectrograph for the region 12 to 330 microns; this basic instrumentation was supplied by Kansas State University.

The initial stages of the research were involved with a test of Burch's law of multiplicative transmittance for mixed absorbing gases when their lines are broadened by H_2 and He, which are constituents of the atmospheres of the major planets. The results, which have resulted in journal publication, indicate that the multiplicative law as originally formulated can be applied with confidence.

The broadening of individual lines in the CO fundamental by various gases has been investigated. The results indicate that the ratio of the "self-broadening ability" of CO to the "line-broadening ability" of foreign gases is greater for lines in the band wings than for lines near the band center when the molecular mass of the broadener is less than that of CO. The results have been interpreted in terms of a phenomenological theory. Studies of the relative line broadening abilities of foreign gases have provided information that can be used to provide optical collision cross sections for individual lines in the CO fundamental.

Other work has been done on the determination of line strength S and half-width for individual CO lines as a function of temperature.

The results at reduced temperatures indicate (1) that line strengths S can be satisfactorily predicted by the Herman-Wallis expression but (2) that at very low temperatures the line half-widths γ differ markedly from values calculated by applying the "hard-sphere" approximations of kinetic theory to values of γ^0 measured at NPT. This work is being continued.

Measurements of total band absorptance $\int A(\nu) d\nu$ as a function of absorber thickness w and total effective pressure P_e have been made at various temperatures T for bands of CO and N₂O. This work is being extended to various other planetary gases.

Attempts have been made to develop a phenomenological theory of line broadening that will adequately account for the phenomena we have observed for the CO fundamental and those reported for more highly polar gases. This theory has been successful in accounting for the variation of line half-width with line number observed in our work on CO and in the studies of HCl-line broadening conducted in other laboratories. The results have been summarized in a journal article.

Laboratory measurements of nitric-acid vapor absorptance have been compared with balloon measurements at the University of Denver in arriving at an estimate of the quantity of nitric acid vapor present in the earth's atmosphere in the region of the ozone layer.

Funds from university sources have been used to purchase a partially completed high resolution spectrograph for use in the region between 2 microns and 5 microns. The instrument has now been completed at Kansas State University. Preliminary tests show that resolution has been reached nearing 50 percent of the Rayleigh limit at amplifier gains and spectrograph slitwidths that can be employed in routine operation.

The high-resolution spectrograph has been used to measure the line strengths and self-broadening parameters in the ν_3 fundamental of CO_2 at laboratory temperature and at a reduced temperature approximating that of the Martian atmosphere. Similar studies have been made for the lines in the CO fundamental for self-broadening and for broadening by CO_2 under conditions similar to those encountered on Mars.

The line strengths S and self-broadening parameters γ^0 of lines in the ν_3 fundamental of N_2O have been measured and compared with earlier values based on earlier S values based on measured band strength and the Herman-Wallis expression and values of γ^0 calculated on the basis of the Anderson theory of line broadening. The results of this study have been incorporated in a doctoral dissertation by L. D. Tubbs.

In view of the importance of ammonia in condensed states in the atmospheres of the Jovian planets, we have attempted to determine the optical constants n_r and n_i of liquid ammonia in the infrared. A paper on the subject has been presented for journal publication.

Cumulative List of Publications*

1. "Further Studies of Overlapping Absorption Bands," Tubbs, Hathaway and Williams, J. Opt. Soc. Amer. 57, 570 (1967) P.
2. "Foreign-Gas Broadening of Absorption Lines in the CO Fundamental," Draegert, Chai, and Williams, J. Opt. Soc. Amer. 57, 570 (1967) P.
3. "Broadening of Absorption Lines in the CO Fundamental," Chai, Draegert, Williams, Bull. Am. Phys. Soc. 12, 542 (1967) P.
4. "Further Studies of Overlapping Absorption Bands," Tubbs, Hathaway, and Williams, App. Opt. 6, 1422 (1967).
5. "Strengths and Half Widths of CO Lines at Reduced Temperatures," Hoover, Hathaway, and Williams, J. Opt. Soc. Amer. 58, 739 (1968) P.
7. "Line Widths in Vibration-Rotation Bands," Williams, Bull. Am. Phys. Soc. II 13, 569 (1968) P.
8. "Comparison for Collision Cross Sections for Line Broadening in the CO fundamental," Chai and Williams, J. Opt. Soc. Amer. 58, 1395 (1968).
9. "Collisional Broadening of CO Absorption Lines by Foreign Gases," Draegert and Williams, J. Opt. Soc. Amer. 58, 1399 (1968).
10. "Absorption in the Wings of Rotational Lines in the CO Fundamental", Chai and Williams, Bull. Am. Phys. Soc. II 13, 906 (1968).
11. "Foreign-Gas Broadening of Lines in the CO Fundamental," Williams, Proceedings 23rd Symposium on Molecular Structure, Ohio State University, p. 89 (1968), P.
12. "Infrared Absorptance of Carbon Monoxide at Low Temperatures," Hoover and Williams, J. Opt. Soc. Amer. 59, 28 (1969).

* P denotes papers presented at scientific meetings.

13. "Nitric-Acid Vapor in the Earth's Atmosphere," Rhine, Tubbs, and Williams, J. Opt. Soc. Amer. 59, 483 (1969) P.
14. "Nitric-Acid Vapor above 19 km in the Earth's Atmosphere," Rhine, Tubbs, and Williams. Applied Optics 8, 1500 (1969).
15. "Half Widths of Collision-Broadened Lines of CO and HCl", Williams, Wenstrand, and Brockman, J. Opt. Soc. Amer. 59, 1526 (1969). P
16. "A Czerny-Turner Spectrograph for the Infrared", Tubbs and Williams J. Opt. Soc. Amer. 60, 726 (1970). P.
17. "Collisional Broadening of Infrared Absorption Lines," Williams, Wenstrand, Brockman, and Curnutte, Molecular Physics 20, 769 (1971).
18. "Collisional Broadening of CO Absorption Lines by CO₂", Tubbs and Williams, J. Opt. Soc. Amer. 61, 673 (1971). P.
19. "Line Strengths and Half-Widths in the ν_3 Fundamental of CO₂", Tubbs and Williams, J. Opt. Soc. Amer. 61, 1587 (1971). P.
20. "Broadening of Infrared Absorption Lines at Reduced Temperatures: CO₂", Tubbs and Williams, J. Opt. Soc. Amer., 62, 285 (1972).
21. "Broadening of Infrared Absorption Lines at Reduced Temperatures: CO", Tubbs and Williams, J. Opt. Soc. Amer., 62, 423 (1972).
22. "Foreign-Gas Broadening of Nitrous-Oxide Absorption Lines", Appl. Opt., 11, 551 (1972).
23. "Reflection and Absorption Spectra of Liquid Ammonia in the Infrared", Charles W. Robertson, Proc. Twenty-Seventh Symposium on Molecular Structure and Spectroscopy (Ohio State University), p.110 (1972).P

24. "The Optical Constants of Liquid Ammonia in the Infrared",
Robertson and Williams, J. Opt. Soc. Am. (Presented for
publication).

II. PROGRESS DURING THIS REPORT PERIOD

A. Absorption-Line Broadening

The papers on absorption-line broadening of CO₂ and CO at telluric and Martian temperatures have been published in the Journal of the Optical Society of America; reprints of the papers are appended. The paper on foreign-gas broadening of N₂O absorption lines has been published in Applied Optics; a reprint of the paper is appended.

New high-resolution work on the strengths and half-widths of lines in the ν_3 fundamental of N₂O has been completed and presented in a doctoral dissertation by L. D. Tubbs.

B. Studies of Particulate Constituents of Planetary Atmospheres

The work on liquid ammonia in the range between 1.6 and 30 micrometers has been completed. An article summarizing the results has been submitted to the Journal of the Optical Society of America; a copy of the manuscript is appended to this report.

III. PERSONNEL

Dr. Dudley Williams, Regents' Professor of Physics:

Chief Investigator (WOC)

Dr. Basil Curnutte, Professor of Physics:

Senior Associate (WOC)

Dr. Charles W. Robertson, Research Associate:

(Part Time)

Lloyd Tubbs, B.S.: Graduate Research Fellow

Graduate Degrees Granted Under the Grant

An-Ti Chai - Ph.D.

Gary M. Hoover - Ph.D.

David Schmieder - M.S.

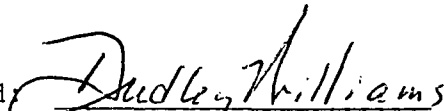
Lloyd Tubbs - Ph.D.

IV. PLANS FOR THE NEXT REPORT PERIOD

- A. The work on N_2O will be continued.
- B. Improvements on the high-resolution instrument will be made with a view to improving its stability at low temperatures.
- C. Preliminary work will be done on solid ammonia.
- D. A conference will be held with Dr. James Pollack and others at the Ames Research Center regarding NASA problems of mutual interest.

Submitted: 22 June 1972

Signed


Dudley Williams

Appendices: (1) - (2) Reprints: "Broadening of Infrared Absorption
Lines at Reduced Temperatures: I. CO_2 , II. CO"

(3) Reprint: "Foreign-Gas Broadening of N₂O
Absorption Lines"

(4) "Optical Constants of Ammonia in the Infrared"

Broadening of Infrared Absorption Lines at Reduced Temperatures: Carbon Dioxide†

LLOYD D. TUBBS AND DUDLEY WILLIAMS

Department of Physics, Kansas State University, Manhattan, Kansas 66502

(Received 29 July 1971)

An evacuated high-resolution Czerny–Turner spectrograph, which is described in this paper, has been used to determine the strengths S and self-broadening parameters γ^0 for lines in the R branch of the ν_3 fundamental of $^{12}\text{C}^{16}\text{O}_2$ at 298 and at 207 K. The values of γ^0 at 207 K are greater than those to be expected on the basis of a fixed collision cross section σ . The approximate ratio of the measured cross sections for a given line is $\sigma(T_1)/\sigma(T_2) = T_2/T_1$; although this relation holds for the average of all lines measured, the cross-section ratio is greater than the temperature ratio for lines near the band center and less than the temperature ratio for lines in the wings of the band.

INDEX HEADINGS: Infrared; Absorption; Spectra.

Carbon dioxide is an important constituent of the atmospheres of Venus, the earth, and Mars. Knowledge of the strengths and widths of its collision-broadened absorption lines in the infrared is important in gaining understanding of the heat balances of the earth and Venus and in making valid estimates of the composition of the extremely thin Martian atmosphere. In earlier studies at ambient laboratory temperatures, Madden¹ determined the strengths and the self-broadening parameters for selected lines in the ν_2 fundamental, and Burch, Gryvnak, and Patty² determined these quantities for the 02⁰3 combination band. If the line strengths at one temperature are known, the line strengths at other temperatures can be calculated.³ However, for the variation of collisional line broadening with temperature, no satisfactory and readily applicable theories have been developed; Goldring and Benesch,⁴ Hoover,⁵ and Ely and McCubbin⁶ demonstrated the failure of the hard-sphere approximation based on simple kinetic theory. The purpose of the present study was to determine the line strengths and self-broadening parameters for lines in the ν_3 fundamental at ambient laboratory temperature and at a reduced temperature comparable with that of the Martian atmosphere.

GENERAL METHOD

The true spectral transmittance of an absorbing gas is given by Lambert's law, $T(\nu) = \exp[-k(\nu)w^0]$, where

$k(\nu)$ is the absorption coefficient and w^0 is the absorber thickness

$$w^0 = p_a z (273/T), \quad (1)$$

where p_a is the partial pressure of the absorbing gas in atm, z is the path length in cm, and T is the Kelvin temperature of the gas. For a collision-broadened line, the absorption coefficient can be approximated⁷ by the Lorentz expression,

$$k(\nu) = S\gamma/\pi[(\nu - \nu_0)^2 + \gamma^2], \quad (2)$$

where ν_0 is the central frequency of the line, γ is the half-width of the line between frequencies at which $k(\nu) = k(\nu_0)/2$, and the line strength $S = \int k(\nu) d\nu$ depends upon the transition probabilities between the initial and final states and upon the populations of these states.

The half-widths of rotational lines under atmospheric conditions are smaller than the spectral slit widths of most ir spectrometers; therefore, the true spectral absorptance $A'(\nu) = 1 - T(\nu)$ is not equal to the measured spectral absorptance $A(\nu)$. However, it has been shown theoretically^{8,9} and experimentally^{7,10} that the equivalent width

$$W = \int A'(\nu) d\nu$$

of an isolated line is within certain limits, independent

of spectral slit width. Utilizing this result, we can write

$$W = \int A'(\nu) d\nu = \int \{1 - \exp[-k(\nu)w_0]\} d\nu$$

$$= \int A(\nu) d\nu, \quad (3)$$

where the limits of integration include the entire range of measurable absorbance associated with the line. For a Lorentzian line, the value of W is given by

$$W = 2\pi\gamma L(x), \quad (4)$$

where $L(x)$ is the Ladenberg-Reiche function¹¹ with argument $x = Sw^0/2\pi\gamma$. Values of $L(x)$ have been tabulated by Kaplan and Eggers¹² for values of x between 0 and 50. However, for certain regions of line growth, W can be approximated by

$$W = Sw^0 \quad \text{for } x \ll 1 \quad (\text{linear region}), \quad (5)$$

$$W = 2(Sw^0\gamma)^{\frac{1}{2}} \quad \text{for } x \gg 1 \quad (\text{square-root region}). \quad (6)$$

In the present study, we have determined line strengths S from measurements in the linear region, in which we used a short absorption cell, small absorber thicknesses w^0 , and large total pressures obtained by the addition of N₂. The product $S\gamma$ was obtained from measurements in the square-root region, in which we used pure CO₂ in a longer cell at pressures sufficiently low to avoid serious overlap of adjacent lines. From the two sets of measurements, we can determine both S and γ ; in the table presented later, we summarize our γ measurements for each line in terms of a single parameter γ^0 , which is equal to the value of γ to be expected for a pure CO₂ sample at a pressure of 1 atm = 1.01×10^6 N/m².

EXPERIMENTAL WORK

In order to determine S and γ^0 by the method just described, it is necessary to use a spectrograph with a sufficiently high resolving power to separate rotational lines, a stable source of radiant flux, and a detector-amplifier system whose output is strictly proportional

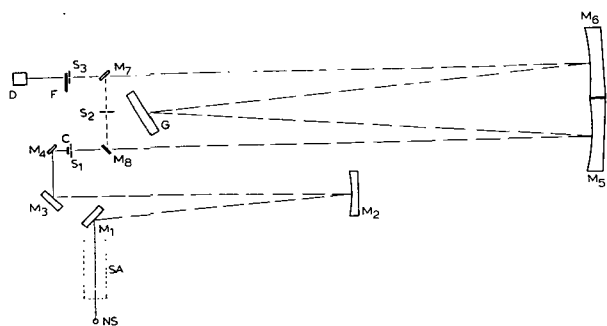


FIG. 1. Schematic diagram of the source assembly and the Czerny-Turner spectrograph.

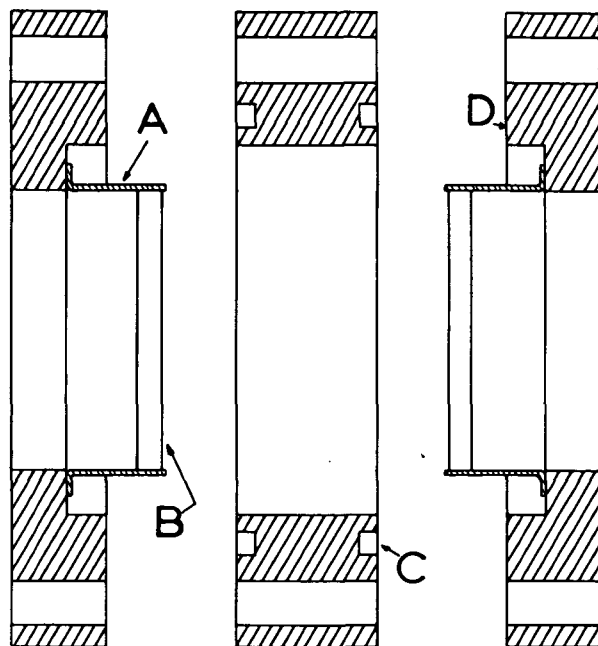


FIG. 2. The components of the absorption cell designed for work at reduced temperatures.

to the flux reaching the detector and which is capable of providing a high signal-to-noise ratio. Commercially available spectrographs equipped with thermocouple detectors are suitable for studies of HCl and CO spectra, in which the rotational lines are widely spaced, but are usually not suitable for larger molecules like CO₂.

The specially constructed, evacuated Czerny-Turner spectrograph used in the present study is shown schematically in Fig. 1. Radiant flux from the Nernst glower NS passes through the sample SA to mirrors M₁, M₂, M₃, and M₄, which produces an image of the source at the entrance slit S₁ of the spectrograph. From S₁, the flux passes to collimating mirror M₅, which directs a collimated beam to the grating G. The dispersed radiation proceeds to condensing mirror M₆, which forms an image of the entrance slit at the intermediate slit S₂ after reflection by M₇. From S₂, the flux is directed by M₈ for a second incidence on the grating and eventual focus at exit slit S₃. The desired flux emerging from S₃ passes through filter F and is directed by an off-axis ellipsoidal mirror, not shown in the figure, to detector D.

System components NS and SA are located in a source tank, which is evacuated by a separate vacuum pump and can be opened without breaking the vacuum in the main tank. After trying out various source control circuits, we ended by operating the Nernst glower in series with a tungsten ballast lamp and utilizing the output of a constant-voltage transformer; the resulting source stability is comparable with that attained by means of more sophisticated techniques. The sample

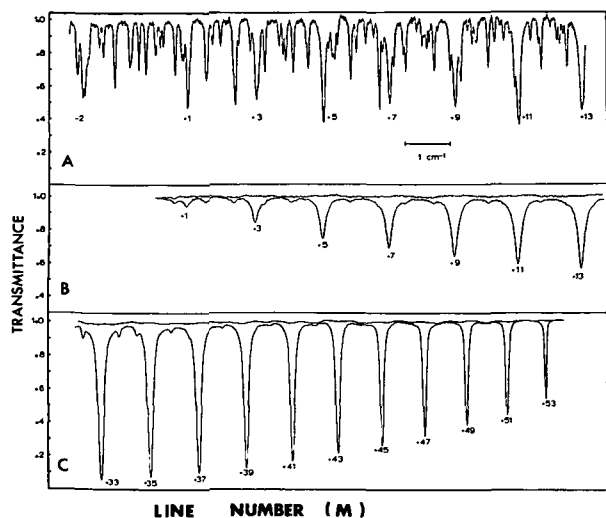


FIG. 3. Typical spectral transmittance curves. Panel A: transmittance of a pure CO_2 sample for a total pressure of 0.18 torr and an effective path length of 2000 cm. Panel B: transmittance of CO_2 at a partial pressure of 3.27 torr in a 0.5-cm cell with N_2 added to give a total pressure of 1 atm. Panel C: transmittance of pure CO_2 at a pressure of 20 torr in a 10-cm absorption cell.

space SA is sufficiently large to accommodate absorption cells 30 cm long.

The construction of the absorption cells is shown schematically in Fig. 2. The cell windows, circular plates B of sapphire 3.8 cm in diameter, were bonded to kovar sleeves A by the Varian's Eimac Division; the kovar sleeves were in turn silver-soldered to heavy copper plates D. The central portions of the absorption cells consist of heavy tubular copper inserts, one of which is shown in Fig. 2. These inserts are equipped with recessed grooves C for use with Teflon-coated cryogenic O-rings supplied by Tec Seal Corporation. The window assemblies are attached to the central portions by means of threaded tie rods passing through holes near the periphery as suggested in Fig. 2. The central inserts are also equipped with copper tubes through which sample gases can be introduced and with small wells into which thermocouples can be inserted for temperature measurements. Thermocouples are also attached to the end plates of the cell.

After the cells had been assembled, they were inserted into close-fitting copper cooling jackets. Cooling was accomplished by circulating cold dry nitrogen through copper tubes which are soft-soldered to the outer surface of the cooling jackets. Cell temperatures were monitored by means of copper-constantan thermocouples attached to the insert portions and end plates of the absorption cells. Temperature gradients in the absorption cells were minimized by proper distribution of cooling tubes on the copper jackets; the jackets extend well beyond the ends of the absorption cells. Cell temperatures were controlled by adjustment of the flow of the cold nitrogen through the coils attached to the cooling jacket.

In passing from SA to M_1 in Fig. 1, the radiant flux passes through a CaF_2 window in the wall of the main vacuum tank and is periodically interrupted at a frequency of 1000 Hz by a tuning-fork-controlled radiation chopper C. Spherical mirrors M_5 and M_6 are 32 cm in diameter and have a focal length of 215 cm. Grating G is an aluminized 15.4 by 20.6-cm Bausch & Lomb replica having 3000 lines/cm with a blaze angle of $35^\circ 52'$ and is used in first order. The grating is rotated by a tangent drive operated by a 5-cm precision micrometer screw supplied by Boeckler Instruments; this relatively short screw can be positioned at different suitable locations by means of a kinematic mounting when different spectral regions are being scanned. The precision screw is advanced by a gear assembly operated by a stepping motor turning at rates as slow as one step in 20 s and as high as 400 steps/s; one step corresponds to a grating rotation of $2 \mu\text{rad}$. For each location of the precision-screw mounting, the grating orientation is indicated by a Veeder counter mounted on a shaft in the gear train operated by the stepping motor. Calibration was accomplished by noting the positions of absorption lines of known frequency on a recorder chart turned by a stepping motor operated from the master control circuit used to rotate the grating; the spectrograph held its calibration for prolonged periods and the grating-rotation mechanism proved to be highly satisfactory.

The main vacuum tank is evacuated by a mechanical pump with a molecular-sieve filter in the pumping line between the pump and the tank; after evacuation to 10^{-2} torr, the pressure inside the isolated tank rose by approximately 0.3 torr in one week. After two years of operation there has been no apparent deterioration of the optical components.

Radiant flux emerging from the spectrograph exit slit S_3 in Fig. 1 is incident on an interference filter supplied by the Optical Coating Laboratory, Inc.; the filter rejected frequencies higher than 3100 cm^{-1} . The off-axis paraboloid brings flux passed by the filter to a focus on a liquid-nitrogen-cooled indium antimonide photovoltaic detector operating with a matched pre-amplifier, supplied by Texas Instruments; the Dewar vessel in which the detector element is mounted can be filled with liquid nitrogen through a copper tube passing through a port in the vacuum tank. The pre-amplifier output signal is further amplified by a Princeton Applied Research narrowband amplifier, whose output is displayed on a recorder chart.

The theoretical resolving power $R = \nu/\Delta\nu$ of the spectrograph is 120 000, where $\Delta\nu$ is the frequency difference corresponding to the diffraction limit at frequency ν . By introducing small quantities of gas at extremely low pressure into the main tank of the spectrograph, we have tested the resolving power by observing closely spaced lines in the spectra of CH_4 , CO_2 , and CO. The measured value of resolving power is 60 000 to 80 000

when the signal-to-noise ratio is acceptable for use in scanning.

In the present study, we used sufficiently large spectral slit widths to ensure large signal-to-noise ratios and confined our attention to the *R* branch of the ν_3 fundamental, because the *P* branch is badly contaminated by weak lines associated with isotopic molecules and hot bands. Typical transmittance curves are shown in Fig. 3, in which panel A shows lines near the center of the band with pure CO₂ at a pressure of 0.18 torr and an effective path length of 2000 cm in the spectrograph tank; the labels on the lines give line numbers $m=J+1$ for lines in the spectrum of the abundant ¹²C¹⁶O₂ molecule, where *J* is the initial rotational level involved in the transition. Panel B represents the spectral absorbance in the same spectral region for CO₂ at a pressure of 3.27 torr in a cell 0.446 cm long when the lines have been pressure broadened by the addition of N₂ to give a total pressure of 1 atm; we note that, although the weaker lines have disappeared as resolved lines, they contribute to the general background absorption and thus add to some extent to the uncertainties of *S* and γ^0 values for lines near the band center. Panel C shows spectral transmittance in the remote wing of the band for a pure CO₂ sample in a 10-cm cell at a pressure of only 20 torr; in this region weak lines make little contribution to the absorbance.

TABLE I. Line strengths *S*, self-broadening parameters γ^0 , and collision cross sections σ for CO₂ at 298 and 207 K.^a

Line number <i>m</i>	<i>S</i> (298 K)	γ^0 (298 K)	σ (298 K)	γ^0 (207 K)	σ (207 K)	σ (207 K)/ σ (298 K)
1 ^b	7.7					
3 ^b	22.8					
5 ^b	37.1					
7	52.3	92	148	202	272	1.84
9	62.1	103	166	190	255	1.54
11	71.2	115	186	198	266	1.43
13	75.7	87	140	179	241	1.73
15	78.0	92	148	172	232	1.57
17	77.7	85	137	157	211	1.54
19	73.1	97	156	181	243	1.55
21	71.3	86	139	143	192	1.38
23	63.8	97	156	172	231	1.47
25	60.0	82	132	149	200	1.51
27	52.6	78	126	155	209	1.65
29	47.1	89	144	167	227	1.57
31	41.4	87	140	130	175	1.25
33	34.2	87	140	143	192	1.37
35	29.8	83	134	119	160	1.19
37	24.8	77	124	119	160	1.29
39	19.7	80	129	138	186	1.44
41	15.8	74	119	129	173	1.45
43	12.5	70	113	109	147	1.30
45	10.2	67	108	98	132	1.22
47	7.56	63	102	88	118	1.15
49	5.80	60	97	83	112	1.15
51	4.60	56	90	86	116	1.29
53	3.25	53	86	81	109	1.27
55	2.24	55	89	91	122	1.37

^a The units employed are as follows: *S* in cm⁻¹/(atm·cm), γ^0 in 0.001 cm⁻¹/atm, and σ in 10⁻¹⁶ cm².

^b The line strengths for these blended lines were calculated on the basis of a band strength $S_0=2040$ cm⁻¹/(atm·cm).

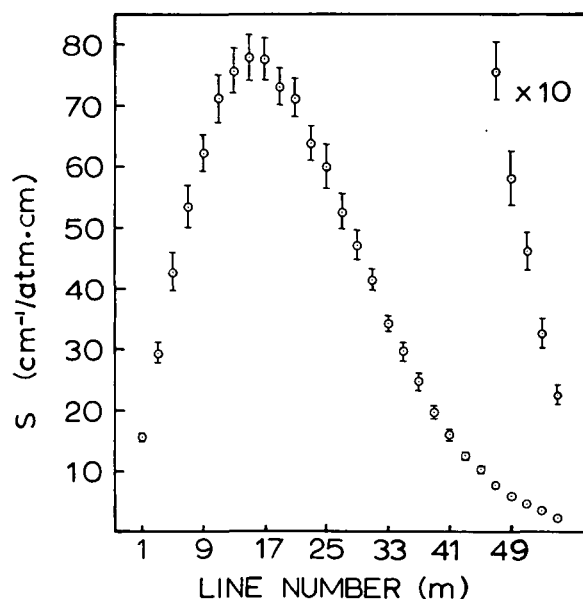


FIG. 4. Measured line strengths *S* for lines in the *R* branch of the ν_3 fundamental of CO₂.

An all-glass manifold was used to handle the samples in the present work; pressures were measured by means of oil and mercury manometers. The gas leads to the sample cells were kept as short as possible.

RESULTS

The results obtained for line strengths S_J (298 K) at room temperature $T_R=298$ K are plotted as a function of line number in Fig. 4 and are listed in Table I. The results are based on measurements with samples for which the Ladenberg-Reiche argument $x<0.2$. The uncertainties are indicated by the error bars in the figure.

The values of *S* in Fig. 4 are directly measured values; however, we note from Fig. 3 that lines $m=1, 3$, and 5 are actually blends of ¹²C¹⁶O₂ lines with weaker lines associated with ¹³C¹⁶O₂ and with hot bands of the abundant isotope. The measured strengths of the blended lines are consistently much larger than those to be expected on the basis of measured strengths of the less-contaminated lines $m=7$ to 55 . The measured strengths of the latter lines yield a band strength $S_0=2040$ cm⁻¹/(atm·cm) when substituted in the Herman-Wallis expression.³ The line strengths listed in Table I for $m=1, 3$, and 5 are values calculated from the Herman-Wallis expression with $S_0=2040$ cm⁻¹/(atm·cm).

Since the combined strengths of the hot bands and ν_3 for ¹³C¹⁶O₂ are approximately 10% that for the ¹²C¹⁶O₂ fundamental, our value of S_0 gives a strength $S_{\text{region}}=2240$ cm⁻¹/(atm·cm) for the entire spectral region. This value is in complete agreement with the Eggers-Crawford value¹³ of 2100 ± 210 cm⁻¹/(atm·cm)

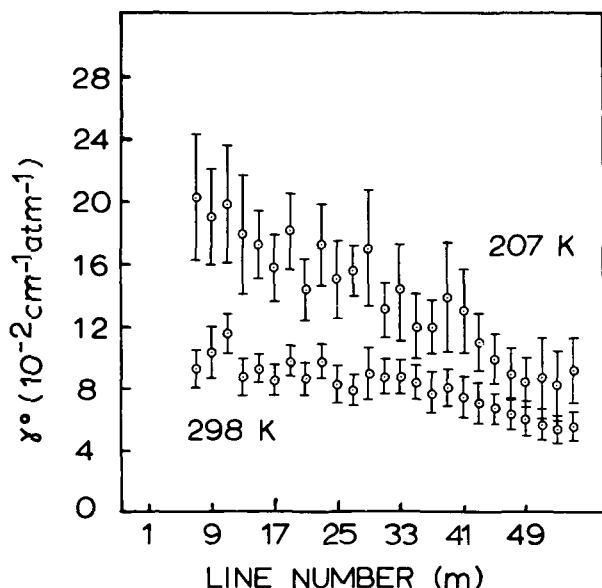


FIG. 5. Measured values of half-width parameter γ^0 for lines in the R branch of the ν_3 fundamental of CO_2 for temperatures of 207 and 298 K. The indicated uncertainty for each point is the sum of the probable error for measurements in the linear region and the probable error for measurements in the square-root region.

for the region and overlaps the value $2500 \pm 400 \text{ cm}^{-1}/(\text{atm} \cdot \text{cm})$ reported by Burch *et al.*¹⁴

Line strengths $S_J(207 \text{ K})$ for the low temperature $T=207 \text{ K}$ were computed from the room-temperature values by use of

$$S_J(207 \text{ K}) = S_J(298 \text{ K})$$

$$\times \frac{Q(298 \text{ K})}{Q(207 \text{ K})} \times \frac{\exp(-E_J/k \times 207 \text{ K})}{\exp(-E_J/k \times 298 \text{ K})}, \quad (7)$$

where Q represents the rotation-vibration partition function at the indicated temperatures and J is the rotational quantum number for the initial rotational level with energy E_J . In using Eq. (7), we assume that the line strengths are directly proportional to the populations of the lower states involved in the transitions and that vibration-rotation interactions are the same at the two temperatures.

The values of the half-width parameters γ^0 obtained at 298 and 207 K are plotted as a function of line number in Fig. 5 and are listed in Table I; the value of γ^0 are based on the $S_J(298 \text{ K})$ values listed in the table together with $S(207 \text{ K})$ computed from Eq. (7) along with measurements of equivalent width in the vicinity of the square-root region with values of $x > 7$. The uncertainty bars in Fig. 5 represent the probable errors of numerous measurements; they are considerably larger for the low-temperature measurements than for the measurements at room temperature.

The chief factors contributing to the uncertainties of S and γ^0 are sampling errors in pressure measurements,

errors in planimetry in obtaining equivalent widths from the recorder charts, errors in temperature measurements, and possible nonlinearities of detector-amplifier response. In the present study, uncertainties of γ^0 as high as 30% are noted for some lines. These uncertainties are to be compared with estimated uncertainties as high as 26% reported by Madden¹ for some lines in the ν_2 fundamental and with estimated uncertainties as high as 11% listed by Burch *et al.*² for the 02⁰³ combination band. Possible nonlinearities in the response of the InSb detector used in the present work cannot be entirely eliminated; Madden employed a Golay cell and Burch used a PbS detector.

We note that, for all lines shown in Fig. 5, γ^0 is greater for samples at 207 K than for samples at 298 K. For lines with $m > 5$, there appears to be a gradual decrease of γ^0 with increasing m at both temperatures. In Fig. 6, we compare the γ^0 values obtained at room temperature by Madden¹ and Burch *et al.*² with those obtained in the present study; in view of the uncertainties involved in the different studies, there seems to be fair agreement. For the three bands studied, the values of γ^0 decrease from approximately $0.12 \text{ cm}^{-1}/(\text{atm} \cdot \text{cm})$ for lines near the band centers to approximately $0.06 \text{ cm}^{-1}/(\text{atm} \cdot \text{cm})$ in the band wings.

DISCUSSION OF RESULTS

On the basis of simple theory, the parameter γ^0 is proportional to the mean collision frequency f_c of a molecule in a sample at atmospheric pressure; thus

$$\gamma^0 = f_c/2\pi = (n\bar{v}\sigma)/2\pi = [n(2kT/\mu)^{1/2}\sigma]/2\pi, \quad (8)$$

where n is the number of molecules per unit volume, $\bar{v} = (2kT/\mu)^{1/2}$ is the mean relative speed of colliding molecules, μ is the reduced mass of the collision pair, and σ is the collision cross section. Because, from the general gas law, $P = nkT$, we note that for the constant-cross-section approximation in which σ is a constant for

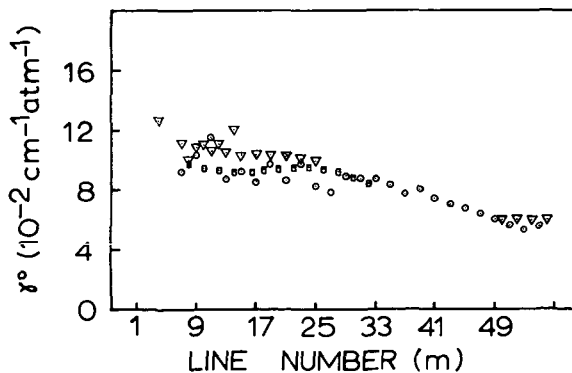


FIG. 6. Self-broadening parameters γ^0 for various rotational lines in CO_2 samples at laboratory temperatures. Present results are given by circles. Madden's results for the ν_2 fundamentals are given by triangles. The results of Burch *et al.* for a combination band are given by the squares.

each line

$$\gamma^0(T_1) \cdot T_1^{\frac{1}{2}} = \gamma^0(T_2) T_2^{\frac{1}{2}} \quad (9)$$

·(constant-cross-section approximation),

where $\gamma^0(T)$ is the half-width parameter for a sample at Kelvin temperature T . Goldring and Benesch⁴ in their studies of HCl, and Hoover and Williams⁵ in studies of CO have noted the failure of the constant-cross-section approximation.

In the present study, Eq. (9) predicts that $\gamma^0(207 \text{ K})/\gamma^0(298 \text{ K}) = (298/207)^{\frac{1}{2}} = 1.2$. Comparison of the measured values of $\gamma^0(207 \text{ K})$ and $\gamma^0(298 \text{ K})$ listed in Table I shows that $\gamma^0(207 \text{ K})/\gamma^0(298 \text{ K}) > 1.2$ for nearly every absorption line; thus we conclude that the constant-cross-section approximation also fails for CO₂.

We have used Eq. (8) to compute the collision cross sections $\sigma(298 \text{ K})$ and $\sigma(207 \text{ K})$ from the measured values of the half-width parameters. The values for these cross sections are listed in Table I along with the ratio $\sigma(207 \text{ K})/\sigma(298 \text{ K})$. We note that the mean value of the ratio $\sigma(207 \text{ K})/\sigma(298 \text{ K}) = 1.44$, which is just the temperature ratio (298 K/207 K) and the standard deviation of ratios for individual lines from the mean is only 0.18. Thus, we might conclude that the collision cross sections are inversely proportional to the absolute temperature,

$$\sigma(T_1) \cdot T_1 = \sigma(T_2) \cdot T_2. \quad (10)$$

However, we note that, despite the small standard deviation, the ratios $\sigma(207 \text{ K})/\sigma(298 \text{ K})$ in Table I do not have truly random variations from the mean ratio. For lines with $m < 19$ near the band center, the ratios are generally higher than the mean, whereas the reverse is true for lines with $m > 31$ in the wing of the band. Thus, we must regard Eq. (9) as only a rough approximation. We note further that the ratios $\sigma(207 \text{ K})/\sigma(298 \text{ K})$ are based on the mean values of measurements involving large probable errors.

It is interesting to compare the present results with Ely and McCubbin's beautiful study⁶ of the P -21 line of 001-100 band of CO₂, in which they used laser radiation tuned to the central frequency of the line and

measured absorption coefficients at numerous temperatures in the range 300-420 K. Within their stated limits of uncertainty, their results are in clear agreement with Eq. (10) in the range 300-380 K but come into some disagreement at higher temperatures. Thus, we must at best regard Eq. (10) as a rough approximation, which depends on the rotational states involved in the transitions.

Yamamoto and his colleagues¹⁵ have recently attempted to apply the Anderson-Tsao-Curnutte theory^{16,17} to the problem of the self-broadening of CO₂ lines. Since their parameters were based largely on the work of Madden, their calculated γ^0 values for 300 K are in full agreement with the γ^0 values plotted in Fig. 6. However, the Yamamoto values of γ^0 at 180 K are in general lower than our measured values of γ^0 at 207 K. Closer agreement might be obtained by further adjustment of the parameters employed in the theory.

REFERENCES

- † Supported in part by a grant from the National Aeronautics and Space Administration. Parts of this paper were presented at meetings of the Optical Society [J. Opt. Soc. Am. **60**, 726A (1970); **61**, 673A (1971); **61**, 1587A (1971)].
- ¹ R. P. Madden, J. Chem. Phys. **35**, 2083 (1961).
 - ² D. E. Burch, D. A. Gryvnak, and R. R. Patty, J. Opt. Soc. Am. **58**, 335 (1968).
 - ³ R. Herman and R. Wallis, J. Chem. Phys. **23**, 637 (1955).
 - ⁴ H. Goldring and W. Benesch, Can. J. Phys. **40**, 1801 (1962).
 - ⁵ G. M. Hoover and D. Williams, J. Opt. Soc. Am. **59**, 28 (1969).
 - ⁶ R. Ely and T. K. McCubbin, Jr., Appl. Opt. **9**, 1230 (1970).
 - ⁷ W. S. Benedict, R. Herman, G. E. Moore, and S. Silverman, Astrophys. J. **135**, 277 (1962).
 - ⁸ J. R. Nielsen, V. Thornton, and E. B. Dale, Rev. Mod. Phys. **16**, 307 (1944).
 - ⁹ H. J. Babrov, J. Opt. Soc. Am. **51**, 171 (1961).
 - ¹⁰ J. N. Howard, D. E. Burch, and D. Williams, J. Opt. Soc. Am. **46**, 186 (1956).
 - ¹¹ R. Ladenberg and F. Reiche, Ann. Physik **42**, 181 (1913).
 - ¹² L. D. Kaplan and D. F. Eggers, J. Chem. Phys. **25**, 876 (1956).
 - ¹³ D. F. Eggers and B. L. Crawford, J. Chem. Phys. **19**, 1554 (1951).
 - ¹⁴ D. E. Burch, D. A. Gryvnak, and D. Williams, Appl. Opt. **1**, 759 (1962).
 - ¹⁵ G. Yamamoto, M. Tanaka, and T. Aoki, J. Quant. Spectrosc. Radiative Transfer **9**, 371 (1969).
 - ¹⁶ P. W. Anderson, Phys. Rev. **76**, 647 (1949).
 - ¹⁷ C. J. Tsao and B. Curnutte, J. Quant. Spectrosc. Radiative Transfer **2**, 45 (1962).

Reprinted from:

JOURNAL OF THE OPTICAL SOCIETY OF AMERICA

VOLUME 62, NUMBER 3

MARCH 1972

Broadening of Infrared Absorption Lines at Reduced Temperatures, II. Carbon Monoxide in an Atmosphere of Carbon Dioxide†

LLOYD D. TUBBS AND DUDLEY WILLIAMS

Department of Physics, Kansas State University, Manhattan, Kansas 66502

(Received 13 September 1971)

The strengths of the rotational lines in the *R* branch of the CO fundamental have been determined at temperatures of 298, 202, and 132 K by means of a high-resolution spectrograph. The results can be used to determine line strengths at other temperatures by means of the Herman-Wallis relation or by considerations of the populations of the rotational levels in the ground vibrational state. Parameters describing the self-broadening and carbon dioxide broadening of CO lines have been determined at 298 and 202 K. The results are compared with other recent experimental and theoretical studies.

INDEX HEADINGS: Infrared; Absorption; Spectra; Atmospheric optics.

Recent spectroscopic studies show that the thin Martian atmosphere consists chiefly of carbon dioxide along with a small quantity of carbon monoxide. In order to make realistic estimates of the amount of CO present from the observed infrared spectra, it is necessary to know the line strengths of CO at Martian temperatures and the broadening of the absorption lines caused by collisions with the more abundant gas CO₂. Although it is possible to make valid computations of line strengths at reduced temperatures from measurements of line strengths at ambient laboratory temperatures, corresponding computations of the widths of absorption lines at reduced temperatures in terms of ambient-laboratory-temperature measurements cannot be made at present, because the molecular optical collision cross sections are not the same at all temperatures and cannot be calculated in any simple way.¹⁻⁴ This variation of collision cross section with temperature presents a currently important problem in molecular physics.

The purpose of the present work was to measure (1) the strengths of lines in the CO fundamental at room temperature and at a Martian temperature with

the purpose of obtaining a set of best values for use in calculations, (2) the corresponding line-broadening parameters γ_{aa}^0 for CO self-broadening, and (3) the corresponding line-broadening parameters γ_{ab}^0 for CO₂ as a foreign-gas broadener. The line-broadening parameter γ^0 is numerically equal to the half-width of the applicable Lorentz line at a pressure of 1 atm; the half-width at other pressures is $\gamma = \gamma^0 p$.

The experimental techniques used in the present work are essentially the same as those employed in our recent study⁴ of CO₂; we shall employ the same terminology in presenting the results of the present study. In the present study we measured CO line strengths *S* at 298, 202, and 132 K and we determined line-broadening parameters γ_{aa}^0 and γ_{ab}^0 at 298 and 202 K. The gases employed were of reagent grade and were supplied by the Matheson Company.

LINE STRENGTHS

The measured line strengths *S* for lines in the *R* branch of CO at a temperature of 298 K are given by the circled points in Fig. 1, which is a plot of *S* as a

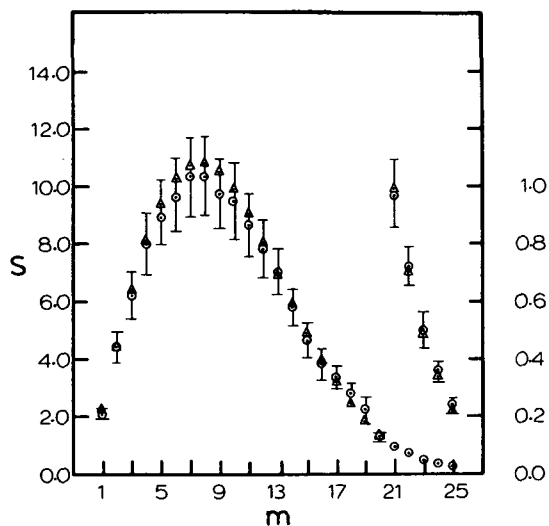


FIG. 1. CO line strengths at 298 K in units of $10^{-2} \text{ cm}^{-1}/(\text{atm cm})_{\text{STP}}$ as a function of line number m . Measured values are shown as circles; values calculated from the Herman-Wallis expression with band strength $S_v=242 \text{ cm}^{-1}/(\text{atm cm})_{\text{STP}}$ are shown as triangles.

function of line number $m=J+1$, where J is the rotational quantum number for the initial level. In this plot S rises to a maximum in the vicinity of $m=7$ and thereafter decreases with increasing m . The points for $m \geq 21$ are replotted on an expanded ordinate scale in the figure.

The points shown as triangles in Fig. 1 represent line strengths calculated from the simplified Herman-Wallis expression⁵

$$S_m = S_v \nu_m |m| \exp[-E_R(m)/kT]/Q_R(T) \cdot \bar{\nu}, \quad (1)$$

where S_v is the total band strength, $E_R(m)$ is the energy of the initial rotational state, Q_R is the rotational partition function for temperature T , and

$$\bar{\nu} = \sum_{m=-\infty}^{m=+\infty} \nu_m |m| \exp[-E_R(m)/kT]/Q_R(T) \quad \text{with } m \neq 0.$$

In this study, we have regarded the band strength S_v as a fitted parameter and have used a computer program to determine the value of S_v that gives the best agreement between the measured and calculated values for the individual line strengths S_m . The value of S_v that gives the best fit for our 298-K data is $242 \text{ cm}^{-1}/(\text{atm cm})_{\text{STP}}$; this value is to be compared with the value $236 \text{ cm}^{-1}/(\text{atm cm})_{\text{STP}}$ used by Benedict *et al.*⁶ We note that all values of S_m calculated from Eq. (1) agree with the corresponding measured values within the limits of experimental uncertainty.

Figure 2 shows line strengths as a function of line number for CO samples at 202 K with measured values shown as circles and calculated values as triangles. Because of the low values of S_m for large m , we have used two ordinate-scale expansions, as indicated in the

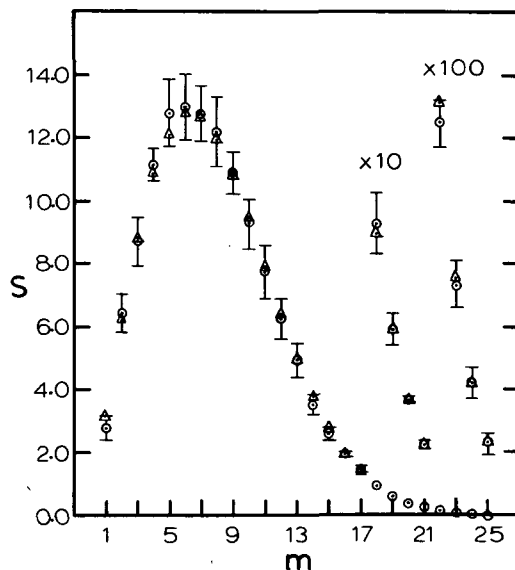


FIG. 2. CO line strengths at 202 K in units of $10^{-2} \text{ cm}^{-1}/(\text{atm cm})_{\text{STP}}$ as a function of line number m . Measured values are shown as circles; values calculated for band strength $S_v=233 \text{ cm}^{-1}/(\text{atm cm})_{\text{STP}}$ are shown as triangles.

figure. The band strength $S_v=233 \text{ cm}^{-1}/(\text{atm cm})_{\text{STP}}$ gives the best fit between measured and calculated line strengths.

The line strengths as a function of line number for gas samples at 132 K are plotted in Fig. 3. For 132 K, the best fit between measured and calculated values is obtained with band strength $S_v=210 \text{ cm}^{-1}/(\text{atm cm})_{\text{STP}}$. The mean value of S_v for the three temperatures is $228 \text{ cm}^{-1}/(\text{atm cm})_{\text{STP}}$; the largest value S_v

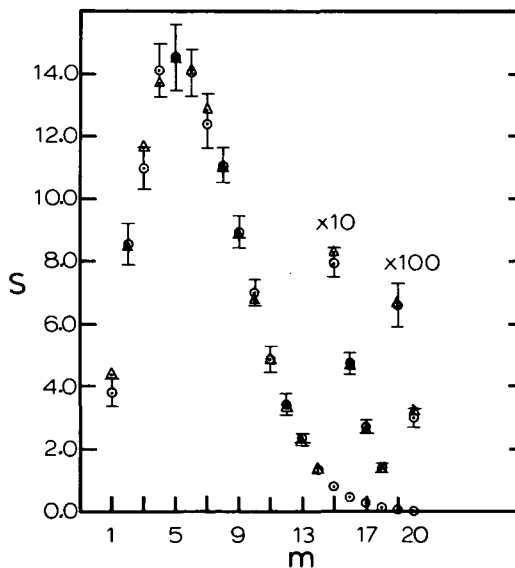


FIG. 3. CO line strengths at 132 K in units of $10^{-2} \text{ cm}^{-1}/(\text{atm cm})_{\text{STP}}$ as a function of line number m . Measured values are shown as circles; values calculated for band strength $S_v=210 \text{ cm}^{-1}/(\text{atm cm})_{\text{STP}}$ are shown as triangles.

TABLE I. Nominal line strengths at 298 K.

m^a	S^b	m	S	m	S
1	2.02	10	9.08	18	2.36
2	4.26	11	8.23	19	1.76
3	5.92	12	7.22	20	1.31
4	7.47	13	6.55	21	0.973
5	8.82	14	5.34	22	0.716
6	9.73	15	4.49	23	0.500
7	10.17	16	3.77	24	0.350
8	10.30	17	3.09	25	0.240
9	9.21				

^a Line number $m = J + 1$ in the R branch.

^b Line strengths S are in units of $\text{cm}^{-1}/(\text{atm cm})_{\text{STP}}$.

is 6% above and the smallest value is 8% below the mean value.

We note that the present best-fit values of S_v decrease monotonically with decreasing temperature. In order to test the possible significance of this, we subjected the earlier data of Hoover and Williams² to a best-fit analysis and obtained S_v values of 213, 225, and 236 $\text{cm}^{-1}/(\text{atm cm})_{\text{STP}}$ at temperatures of 300, 193, and 153 K, respectively. Because this variation with temperature is just the reverse of that obtained in the present study, we can report no significant systematic change of S_v with temperature.

The purpose of the present line-strength measurements was to provide data from which line strengths at reduced temperatures can be calculated. We have used the present measurements along with those of Hoover and Williams² and Benedict *et al.*⁶ as basic data for two sets of calculations; these data are supported by some 740 individual line measurements in the present study, 414 measurements in the Hoover-Williams study, and a comparably large number of measurements in the Benedict study.

One method of calculation is based on the simplified Herman-Wallis relation given in Eq. (1), in which vibration-rotation interactions are omitted. With the use of a nominal band strength $S_v = 228 \text{ cm}^{-1}/(\text{atm cm})_{\text{STP}}$, we find that the rms deviation of the observed line strengths S_m from the calculated line strengths is 8.4%. Thus, for the existing data, we find that Eq. (1)

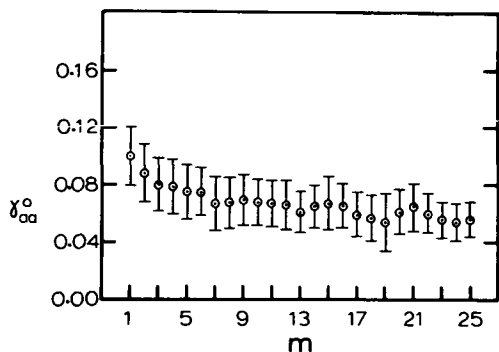


FIG. 4. Measured self-broadening parameters for CO at 298 K in units of $\text{cm}^{-1}/\text{atm}$ as a function of line number.

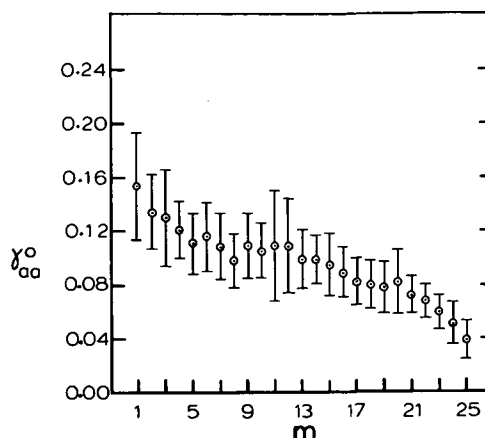


FIG. 5. Measured self-broadening parameters for CO at 202 K in units of $\text{cm}^{-1}/\text{atm}$ as a function of line number.

can be used to good approximation in calculating S_m . The poorest agreement between observed and calculated values was noted at 132 K. Equation (1) with $S_v = 228 \text{ cm}^{-1}/(\text{atm cm})_{\text{STP}}$ should be used with caution in computing line strengths at elevated temperatures because rotation-vibration interactions may be appreciable for large values of m .

A second scheme for determining line strengths at various reduced temperatures can be based on the fact that the strength of a rotational line in the CO fundamental is directly proportional to the population of the initial rotational level. Thus, if line strength S_m is known at 298 K, the strength of the same line at temperature T can be determined from the relation

$$\frac{S_m(T)}{S_m(298 \text{ K})} = \frac{\exp(-E_J/kT)/Q_R(T)}{\exp[-E_J/k(298 \text{ K})]/Q_R(298 \text{ K})}, \quad (2)$$

where E_J is the energy of the initial rotational state and Q_R is the rotational partition function at the indicated temperatures. We have used the existing data to obtain a set of nominal values of $S_m(298 \text{ K})$ for use in Eq. (2) for prediction of S_m at other temperatures. By use of the nominal S_m values listed in Table I, we find that the rms deviation of measured values from the predicted values is 7.3%. Thus, Eq. (2) provides a slightly better fit to the existing data than Eq. (1) with a single value for S_v .

Equation (2) can also be used to predict S_m values at elevated temperatures for the lines listed in Table I, provided that the vibrational partition function is introduced; it gives no information for lines for $m > 25$, for which we have not determined nominal S_m values at 298 K.

COLLISIONAL BROADENING

The measured values of line-broadening parameters are shown graphically as a function of line number in Figs. 4-8. Each point in these plots is based on eleven

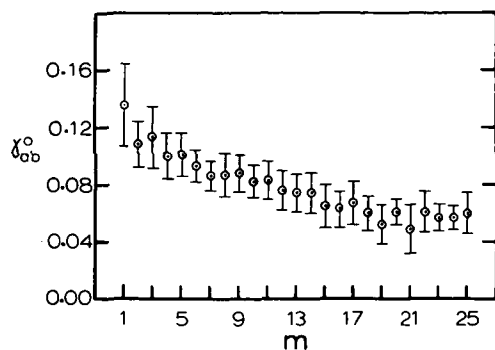


FIG. 6. Parameters for broadening of CO lines by CO₂ at 298 K in units of cm⁻¹/atm as a function of line number.

independent determinations. Although the experimental uncertainties indicated in the figures are somewhat larger than the uncertainty estimates in some earlier lower-resolution work summarized by Hoover,² the use of a high-resolution spectrograph has resolved certain paradoxes involving the widely differing values reported earlier for the γ^0 values at 300 K for line $m=1$. This line is actually a blend with the $m=15$ absorption line of the isotopic molecule ¹³CO; although the ¹³CO line contributes little to the measured line strength, its contribution to the measured γ^0 values can be important.⁷ After correction for the blended line, our present results for $m=1$ at 298 K give

$$\gamma_{aa}^0 = 0.101 \text{ cm}^{-1}/\text{atm}$$

and at 202 K give

$$\gamma_{aa}^0 = 0.154 \text{ cm}^{-1}/\text{atm}.$$

The present results for the influence of temperature on the self-broadening parameter γ_{aa}^0 are in general agreement with the earlier results of Hoover,² which covered the range $m=1$ to 21. Both investigations showed that the ratio of γ_{aa}^0 at approximately 200 K to γ_{aa}^0 at approximately 300 K decreases from approxi-

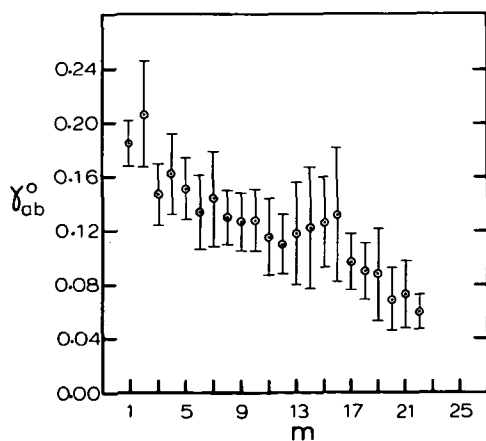


FIG. 7. Parameters for broadening of CO lines by CO₂ at 202 K in units of cm⁻¹/atm as a function of line number.

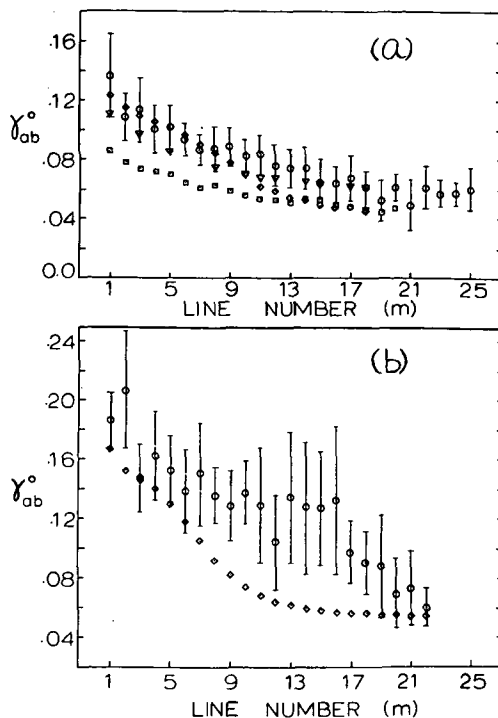


FIG. 8. Comparison of present values of parameters for CO₂ broadening of CO absorption lines with those obtained in earlier studies. (a) The parameters for broadening at approximately 300 K; present results are given by circled points, those of Varanasi by diamonds, those of Draeger and Williams by triangles, and those of Crane-Robinson and Thompson by squares; (b) the parameters for broadening at approximately 200 K. The present results are given by circled points; the values computed by Varanasi and Tejwani on the basis of the Anderson-Tsao-Curnutte theory are given by diamonds.

mately 1.6 for low m values to nearly unity in the vicinity of $m=20$. In the present work we find that the ratio is less than unity for $m>22$; this result is consistent with Hoover's results at $T=124$ K, at which temperature the parameters γ_{aa}^0 for $m>14$ are smaller than the corresponding parameters at 300 K. For the temperatures 202 and 298 K used in the present study, the ratio $\gamma_{aa}^0(202 \text{ K})/\gamma_{aa}^0(298 \text{ K})=1.2$ is predicted on the basis of the constant-collision-cross-section approximation; the failure of this approximation is obvious.

Our results for the parameter γ_{ab}^0 for broadening of CO lines by CO₂ at 298 and 202 K are plotted in Figs. 6 and 7, respectively. After corrections for the ¹³CO blended line, the values $\gamma_{ab}^0=0.136 \text{ cm}^{-1}/\text{atm}$ at 298 K and $\gamma_{ab}^0=0.186 \text{ cm}^{-1}/\text{atm}$ at 202 K are obtained for $m=1$. The 298-K results in Fig. 6 indicate a gradual decrease of γ_{ab}^0 with increasing line number m ; the ratio of γ_{ab}^0 for the lowest m values to γ_{ab}^0 for the highest m values is approximately 2. The values of γ_{ab}^0 at 202 K plotted in Fig. 7 show a much more rapid decrease with increasing m ; the ratio of γ_{ab}^0 for the lowest m values to γ_{ab}^0 for the highest m values is approximately 3. The plotted values of γ_{ab}^0 in Fig. 7 actually show a slight increase as m increases from 12

to 16; however, in view of the large experimental uncertainties, no significance can be attached to the apparent hump in the plot near $m=16$. We note that the ratio $\gamma_{ab}^0(202\text{ K})/\gamma_{ab}^0(298\text{ K})$ ranges from nearly 2 for some m values to slightly more than unity at $m=22$ and averages approximately 1.5; the constant-collision-cross-section approximation again predicts a ratio of 1.2 for all lines.

It is perhaps of interest to compare the parameters for CO₂ broadening with those for CO self-broadening at the two temperatures covered in the present work. At 298 K, the ratio $\gamma_{ab}^0/\gamma_{aa}^0$ ranges from approximately 1.3 for $m=1$ to 5 to approximately unity for $m>20$. At 202 K, the ratio also ranges from approximately 1.3 for $m=1$ to 5 to approximately unity near line $m=21$.

DISCUSSION OF RESULTS

As we have indicated earlier, our results for CO self-broadening are in general agreement with those obtained by Hoover and Williams,² who have given a detailed comparison of their values of γ_{aa}^0 at 300 K with the results of earlier investigations. Our present values of γ_{aa}^0 at 298 K are in somewhat closer agreement with the more recent values of Burch and Gryvnak⁸ and Kostkowski and Bass⁹ than with those reported by earlier investigators.^{10,11}

A comparison of our present values of γ_{ab}^0 for broadening by CO₂ at ambient laboratory temperature with those of other investigators is given in Fig. 8(a). For the range $m=1$ to 8, the present values are in excellent agreement with recent experimental results reported by Varanasi¹²; for the range $m=9$ to 18, the present values of γ_{ab}^0 are higher than those reported by Varanasi. There is fair agreement between the present results and those of Draegert and Williams¹³ over most of the range of m ; the present values of γ_{ab}^0 are consistently higher than those reported by Crane-Robinson and Thompson.¹⁰

Although no values of γ_{ab}^0 at 200 K are available for comparison with our present results, we can make a comparison with a set of calculated values. Varanasi and Tejwani¹⁴ have applied the Anderson-Tsao-Curnutte (ATC) theory to the problem of the broadening of CO lines by CO₂. For a temperature of 295 K, their computed values of γ_{ab}^0 are in excellent agreement with Varanasi's experimental values¹² over the entire range $m=1$ to 18. These authors have also attempted to use the ATC theory in calculating γ_{ab}^0 at reduced temperatures.

Figure 8(b) shows a comparison of our present experimental values of γ_{ab}^0 with the calculated values

of Varanasi and Tejwani. The calculated values are in general lower than our measured values but fall within our limits of experimental uncertainty for lines $m=1, 3, 4, 5, 6, 19, 20, 21,$ and 22 . The differences between the observed and calculated values is greatest in the intermediate region $m=7$ to 18 .

We recognize that the present work represents merely a first step in an understanding of the broadening of CO by CO₂ at Martian temperatures and have given conservatively large estimates of uncertainty; in view of the disagreements between earlier independent investigations of CO self-broadening at 300 K, we hope that other investigators will check our present measurements in the near future.

In order to provide data for comparison with ATC calculations it is desirable to undertake measurements of γ_{ab}^0 for broadening of CO by various simple gases as a function of temperature. Although the results of such studies would not have direct planetary applications, they might prove highly useful in the development of readily and widely applicable theories. Even relative measurements of line broadening as a function of temperature, which can usually be more precise than absolute measurements, could prove useful in providing tests of the validity of the ATC theory.

REFERENCES

† Work supported in part by the National Aeronautics and Space Administration.

- ¹ H. Goldring and W. Benesch, *Can. J. Phys.* **40**, 1801 (1962).
- ² G. M. Hoover and D. Williams, *J. Opt. Soc. Am.* **59**, 28 (1969).
- ³ R. Ely and T. K. McCubbin, Jr., *Appl. Opt.* **9**, 1230 (1970).
- ⁴ L. D. Tubbs and D. Williams, *J. Opt. Soc. Am.* **62**, 284 (1972).
- ⁵ R. Herman and R. F. Wallis, *J. Chem. Phys.* **23**, 637 (1955).
- ⁶ W. S. Benedict, R. Herman, G. E. Moore, and S. Silverman, *Astrophys. J.* **135**, 277 (1962).
- ⁷ In the S determinations, measurements are made in the linear region of line growth; if the ¹²CO line is in the linear region, the ¹³CO line is also in the linear region. The γ^0 determination is made in the square-root region of line growth; even if the ¹²CO line is in the square-root region, the ¹³CO line may not be in this region. In correcting for the ¹³CO line we have made use of tabulated values of the Ladenberg-Reiche function and have assumed no overlapping.
- ⁸ D. E. Burch and D. A. Gryvnak, *J. Chem. Phys.* **47**, 4930 (1967).
- ⁹ H. J. Kostkowski and A. M. Bass, *J. Quant. Spectrosc. Radiative Transfer* **1**, 117 (1961).
- ¹⁰ C. Crane-Robinson and H. W. Thompson, *Proc. Roy. Soc. (London)* **A272**, 441 (1963); **A272**, 453 (1963).
- ¹¹ R. H. Hunt, R. A. Toth, and E. K. Plyler, *J. Chem. Phys.* **49**, 3909 (1968).
- ¹² P. Varanasi, *J. Quant. Spectrosc. Radiative Transfer* **11**, 249 (1971).
- ¹³ D. A. Draegert and D. Williams, *J. Opt. Soc. Am.* **58**, 1399 (1968).
- ¹⁴ P. Varanasi and G. D. T. Tejwani, *J. Quant. Spectrosc. Radiative Transfer* **11**, 255 (1971).

Foreign-Gas Broadening of Nitrous Oxide Absorption Lines

Lloyd D. Tubbs and Dudley Williams

We have measured the foreign-gas broadening coefficients for collisional broadening of lines in the ν_3 fundamental of N_2O by He, Ne, Ar, Kr, Xe, H_2 , D_2 , and CH_4 . These coefficients, which give the ratio of the line-broadening ability of these gases to the line-broadening ability of N_2 , can be used with recent measurements and calculations of N_2 broadening to obtain optical collision cross sections.

Introduction

Earlier studies¹ of the total band absorptance of telluric gases whose absorption lines are collisionally broadened by nitrogen have shown that the equivalent width of a band can be expressed in terms of absorber thickness w and an effective pressure

$$P_e = Bp_a + p_N, \quad (1)$$

where p_N is the partial pressure of nitrogen, p_a is the partial pressure of the absorbing gas, and the self-broadening coefficient B is the ratio of the line-broadening ability of the absorbing gas to the line-broadening ability of nitrogen. If a gas other than nitrogen is used as a broadener, the effective or nitrogen-equivalent pressure can be written

$$P_e = Bp_a + Fp_b, \quad (2)$$

where p_b is the partial pressure of the broadening gas and the foreign-gas broadening coefficient F is the ratio of the line-broadening ability of the broadening gas to that of nitrogen. Values of F appropriate for use with entire bands have been reported by Burch *et al.*²

In more recent studies Anderson *et al.*³ have determined self-broadening coefficients $B(\nu)$ appropriate for various frequencies ν within the major absorption bands of various atmospheric gases. Chai and Williams⁴ have determined $B(\nu)$ for individual lines in the R branch of the CO fundamental, and Draegert and Williams⁵ have made corresponding measurements of $F(\nu)$ for various foreign gases.

Present Study

The present study is concerned with the determination of $F(\nu)$ values for various foreign gases for lines in the ν_3 fundamental of N_2O . The general procedure in-

volves first the introduction of a small carefully measured quantity of N_2O into an absorption cell of length $l = 5$ cm to give a relatively small absorber thickness $w \sim p_a l$ and then the mapping of the absorption spectrum. Addition of a broadening gas to the original gas increases spectral absorption $A(\nu)$ as a result of line broadening. The lower curve in Fig. 1 shows the spectral absorption at a given frequency as a function of the partial pressure p_N of added nitrogen; the upper curve in Fig. 1 shows spectral absorption for the same absorber thickness of N_2O as deuterium gas is added. For any particular value of fractional spectral absorption given by the ordinate in Fig. 1 the F value of the deuterium broadener is given by the ratio of pressures; i.e., $F = p_N/p_b$, where p_N and p_b are the corresponding partial pressures given by the abscissa in Fig. 1. We note that the best values of F are obtained from the ratios for which the pressures of the broadening gases are sufficiently large to provide reliable separations of the curves but sufficiently low to avoid saturation effects.

A Perkin-Elmer model 421 spectrograph was used with spectral slit widths sufficiently wide to include several adjacent spectral lines. In his CO studies Draegert⁵ found that the F values obtained with wide spectral slit widths are essentially the same as those obtained with narrow slits in spectral regions where the spectral absorption is not changing rapidly; for most of the CO fundamental, smooth curves drawn through F values obtained for individual lines coincide with the curves through the points giving the F values obtained with broader slits when both curves are plotted as a function of frequency. Exceptions to this result were noted at the band center and in the remote wings of the band, where the spectral absorption is changing rapidly with frequency. We have used this spectral averaging property of the spectral slit width in the present study.

The gases used in the present work were of reagent grade and were supplied by the Matheson Company. All pressures were measured by suitable manometers

The authors are with the Physics Department, Kansas State University, Manhattan, Kansas 66502.

Received 6 August 1971.

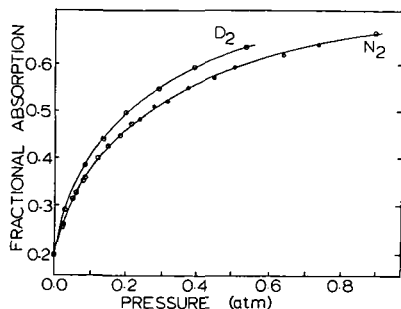


Fig. 1. Measured spectral absorption at a given frequency for a given absorber thickness of N_2O as a function of the partial pressure of the line-broadening gases D_2 and N_2 .

attached to a gas-handling manifold similar to those used in previous studies.

Results

The experimental results obtained in the present investigation are summarized in Fig. 2. Panel A of this figure shows the spectral transmission of a sample of pure N_2O as observed with the broad spectral slits employed in the course of the work. We note that although the dominant absorption in the indicated spectral region is associated with the ν_3 fundamental of $N_2^{14}O^{16}$, the actual absorption spectrum is not simple. Whereas the R branch is relatively *clean*, the P branch is badly *contaminated* by weak lines associated with the ν_3 fundamental of various isotopic species and by the somewhat stronger lines of hot bands associated with molecules initially in the first excited state of ν_2 .

Plots of measured F values as a function of frequency are given in panels B, C, and D of Fig. 2. We note that the F values for H_2 have their minimum values for lines near the center of the major ν_3 band and rise rapidly in the P and R branches; the sudden decrease in $F(\nu)$ suggested by the final points in the extreme wings is probably an artifact associated with the failure of our broad slit-width technique. The plots of $F(\nu)$ vs ν for D_2 and He also show minima near the band center with generally increasing values in the P and R branches and attaining nearly constant or even slightly decreasing values in the remote wings.

For Ne the F value remains nearly constant at the low value of 0.6 throughout the entire band. In contrast to Ne, the Ar, Kr, and Xe plots indicate a decrease in $F(\nu)$ as one proceeds from the band center through the P and R branches into the wings of the band. The decrease is least for Ar and greatest for Xe.

For the larger polyatomic molecule CH_4 , the $F(\nu)$ values fall in the range 1.2–1.3 throughout the entire band.

Discussion of Results

If we assume that our measured values of $F(\nu)$ are indeed valid measures of F for individual rotational lines in the vicinity of ν , we note that $F(m)$ increases with increasing line number m for H_2 , D_2 , and He,

where $m = J + 1$ in the R branch and $m = J$ in the P branch, and J is the rotational quantum number of the lower level involved in the transition. We note further that $F(m)$ does not vary appreciably with m for CH_4 or Ne and that $F(m)$ decreases with increasing m for Ar, Kr, and Xe. The present results for the monatomic and diatomic broadeners are similar to earlier results for CO^5 and to the results obtained by others in studies of the foreign-gas broadening of the rotational lines of CO and HCl; these earlier results have been summarized by Williams *et al.*,⁶ who note a connection between the $F(m)$ vs m variation and the reduced mass μ_{ab} of the absorbing and broadening molecules constituting the collision pair; the $F(m)$ values increase with increasing m for $\mu_{ab} < \mu_{aN}$ but decrease with increasing m for $\mu_{ab} > \mu_{aN}$.

In order to use the measured F values in making theoretical estimates of transmission, it is convenient to make use of the Lorentz model of absorption lines and apply the Ladenberg-Reiche⁷ function $L(x)$, which provides a measure for the equivalent width $\int A(\nu) d\nu$ of a line; the argument $x = Sw^0/2\pi\gamma$, where w^0 is the absorber thickness, S is the line strength, and γ is the half-width of the collision-broadened line. Kaplan and Eggers⁸ have tabulated the values of $L(x)$ over wide ranges of the argument. The line strength depends on the quantum-mechanical transition probability for transitions between the initial and final states and upon the populations of these states; at a given sample

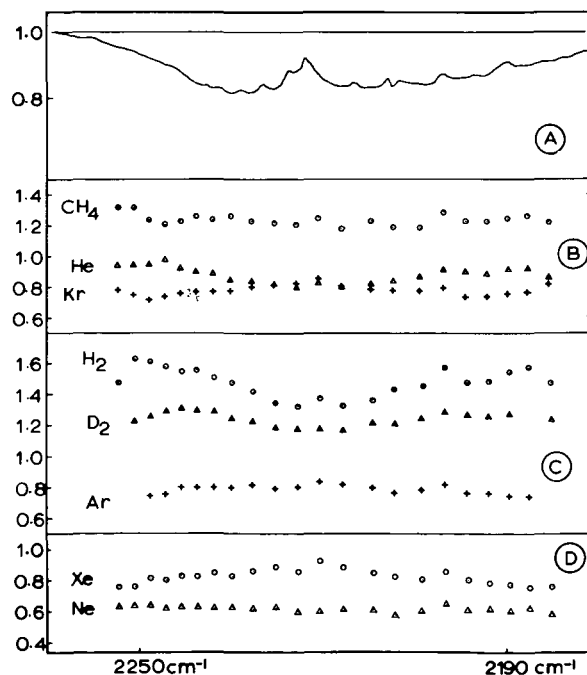


Fig. 2. Panel A shows spectral transmittance of a pure N_2O sample as observed with the broad spectral slit width employed in determining $F(\nu)$. Panels B, C, and D show measured values of $F(\nu)$ for various gases as a function of frequency; we estimate that except for values in the extreme wings of the band, the values of $F(\nu)$ given by the points have an uncertainty of $\pm 5\%$.

temperature, S is independent of pressure for pressures as high as several atmospheres. The half-width γ depends upon the mean molecular-collision frequency and is therefore directly proportional to the pressure at a given temperature.

According to simple theory, $\gamma = f_c/2\pi$, where the mean collision frequency $f_c = n\bar{v}\sigma$, n is the number of molecules per unit volume, \bar{v} is the mean relative speed of the colliding molecules, and σ is the collision cross section. Making use of the general gas law $p = nkT$ and the expression $\bar{v} = (2kT/\mu)^{1/2}$, where μ is the reduced mass of the collision pair, we may write for gas samples at the same temperature:

$$\sigma_{ab} = F(\mu_{ab}/\mu_{aN})^{1/2}\sigma_{aN}, \quad (3)$$

where σ_{ab} is the cross section for collisions between the absorbing molecule and broadening molecule b and σ_{aN} is the cross section for collisions between the absorbing molecule and nitrogen molecules. Once the cross sections are known, line half-widths can be determined for any pressure at the temperature in question.

Thus far, σ_{aN} values for lines in the ν_3 fundamental have not been determined by direct curve-of-growth measurements for N_2O-N_2 collisions. However, Tejwani and Varanasi⁹ have used the Anderson-Tsao-Curnutte theory to compute γ_{aN} and hence σ_{aN} for N_2O-N_2 collisions at laboratory temperature and have compared their results with estimates based on earlier experiments as summarized by Goldman *et al.*¹⁰ The computed values of σ_{aN} agree best with values based on Goody's recent work¹¹ on N_2O bands near $3.9 \mu m$. If the calculated values of σ_{aN} are accepted, the values of $F(m)$ obtained in the present work can be used to compute σ_{ab} for collisions between N_2O and the broadening gases covered in the present investigation.

Tejwani and Varanasi⁹ have pointed out that direct curve-of-growth measurements of line broadening for N_2O can be made with a spectrometer having a resolu-

tion of 0.05 cm^{-1} or less. Preliminary tests indicate that our recently constructed spectrograph may indeed prove satisfactory for the purpose; we have recently obtained reasonably satisfactory results for CO_2 lines¹² which have twice the spacing of N_2O lines. It is also possible that deconvolution techniques for collisionally broadened lines can be developed to obtain line widths directly from spectral chart recordings.

Although we did not obtain $F(\nu)$ values for O_2 in the present study, an earlier study² of total band absorption gave an O_2 F value of 0.83 for the ν_3 band and 0.72 for the ν_1 band. These measured values are to be compared with the corresponding value of approximately 0.6 that is obtained by taking the ratio of the calculated line widths given by Tejwani and Varanasi.

This work was supported in part by the National Aeronautics and Space Administration.

References

1. D. E. Burch and D. Williams, *Appl. Opt.* **1**, 587 (1962).
2. D. E. Burch, E. B. Singleton, and D. Williams, *Appl. Opt.* **1**, 359 (1962).
3. A. Anderson, A. T. Chai, and D. Williams, *J. Opt. Soc. Am.* **57**, 240 (1967).
4. An-Ti Chai and D. Williams, *J. Opt. Soc. Am.* **58**, 1395 (1968).
5. D. A. Draeger and D. Williams, *J. Opt. Soc. Am.* **58**, 1399 (1968).
6. D. Williams, D. C. Wenstrand, R. J. Brockman, and B. Curnutte, *Mol. Phys.* **20**, 769 (1971).
7. R. Ladenberg and F. Reiche, *Ann. Phys.* **42**, 181 (1913).
8. L. D. Kaplan and D. F. Eggers, *J. Chem. Phys.* **25**, 876 (1956).
9. G. D. T. Tejwani and P. Varanasi, *J. Quant. Spectrosc. Radiative Transfer* **11**, 1659 (1971).
10. A. Goldman, D. G. Murcray, F. H. Murcray, W. J. Williams, T. G. Kyle, and J. N. Brooks, *J. Opt. Soc. Am.* **60**, 1466 (1970).
11. R. M. Goody, *J. Opt. Soc. Am.* **58**, 904 (1968).
12. L. D. Tubbs and D. Williams, *J. Opt. Soc. Am.* **62** (in press, 1972).

The Optical Constants of Liquid Ammonia in the Infrared*

Charles W. Robertson and Dudley Williams

Department of Physics, Kansas State University, Manhattan, Kansas 66502

Abstract

On the basis of quantitative studies of spectral reflectance in the range $5100\text{-}350\text{ cm}^{-1}$ and spectral transmittance between 7000 and 875 cm^{-1} we have determined the real and imaginary parts of the refractive index of liquid ammonia in the spectral region in which the two sets of measurements overlap. We have also determined these optical constants in the range $5000\text{-}350\text{ cm}^{-1}$ from a Kramers-Kronig analysis of the reflectance measurements. The results of the investigation are presented in graphical and tabular form.

Introduction

In view of the presence of ammonia in the cloud cover of the Jovian planets, a detailed knowledge of the optical constants of ammonia in condensed states is important to studies of the radiative energy balances of these planets. Recent studies of liquid ammonia have included a precise determination of its refractive index in the spectral vicinity of the D lines of sodium¹ and two studies of its infrared absorption spectrum.^{2,3} In the present study we have determined the real n_r and imaginary n_i parts of its refractive index in the infrared.

Reflection Measurements

Figure 1 gives a schematic diagram of the reflectometer employed. Radiant flux from the Nernst glower N is reflected by concave mirror M_1 and plane mirror M_2 , which produce a magnified image of the glower at I_1 . The flux is then reflected by plane mirror M_3 to concave mirror M_4 , which produces a still further magnified image I_2 at the surface of the liquid ammonia sample or the horizontal surface of a reference mirror. After reflection by the test surface, the flux reaches concave mirror M_5 and plane mirror M_6 , which produce a final image I_3 at the entrance slit of a Perkin-Elmer Model 112 spectrometer; final image I_3 is twice the size of the Nernst glower. The reflectometer was designed to give an under-fill of the spectrometer's optical system.

The angle of incidence of the central ray at the sample surface was 5° ; the angles of incidence for the extreme rays in the converging flux cone were 9° and 1° . Thus, conditions for near-normal incidence were closely approximated. Image I_2 at the sample surface had a linear magnification of 6,

relative to the glower; the use of this enlarged image minimized difficulties due to localized heating at the sample surface. With I_2 at the sample surface, small surface waves can alter the fill of mirror M_5 but have negligible effect on the position of the final image I_3 ; by making mirror M_5 larger than the mirror needed to accept all flux reflected from a quiescent sample surface we attempted to eliminate the effects of surface waves, which are produced by building vibrations even in our basement laboratory. Having distance I_2-M_5 greater than distance M_5-I_3 reduces defocussing effects due to changes in the liquid surface caused by evaporation.

The liquid ammonia sample S in a shallow glass dish D and the reference mirror M were housed side by side at the bottom of a pair of communicating stainless-steel wells W mounted inside a hollowed block P of polystyrene foam in the manner suggested by Fig. 2. The sample and reference mirror were positioned in this way in an effort to equalize the amount of ammonia vapor in sample and reference paths and thus to compensate for absorption by ammonia vapor. The polystyrene-foam block was mounted on a cart providing lateral motion for positioning either the sample or the reference mirror at I_2 in Fig. 1. This cart was housed in a plywood box from which the ammonia was gently removed by an exhaust fan and vented outside the building.

The ammonia was Air Products' anhydrous grade and was taken directly from the tank without further purification. Ammonia in the dish D in Fig. 2 was cooled to $-45^{\circ} \pm 2^{\circ}\text{C}$ by rapid evaporation and remained at this low temperature while measurements were being made. While the sample dish was being filled, an aluminum baffle was inserted between the wells in order

to protect the aluminized mirror surface. Although liquid condensates were formed on the cold well walls, no identifiable spectroscopic difficulties were encountered as a result of contamination of the sample by condensation of atmospheric water vapor. In order to inhibit condensation on the reference mirror, we kept the temperature of the mirror somewhat above the temperature of the surrounding walls; dissipation of only 3.5 watts in resistors H was sufficient to prevent condensation. We detected no changes in the spectral reflectance of ammonia during the useful life of a sample.

The techniques used in mapping spectral reflectance were essentially the same as those used in our earlier study of water.⁴ Since the reflectance of ammonia is small compared with that of the reference mirror, we used a rapidly rotating calibrated sector wheel to attenuate the flux reflected by the mirror so that, without change in amplifier gain settings, we could compare sample and mirror reflectance from pen deflections on a recorder chart. An auxiliary He-Ne laser was used to advantage during leveling adjustments of the reference mirror to the horizontal. The absolute reflectance of the reference mirror was measured from time to time by means of an auxiliary Strong reflectometer.⁵

The spectral reflectance curve in Fig. 3 is the smoothed result of the average of 3 to 10 reflectance measurements taken at each of 220 different frequencies. The reflectance curve shows typical dispersion features in the vicinity of strong absorption bands near 3300, 1630, and 1058 cm^{-1} and appears to reach a maximum at 350 cm^{-1} , the lowest frequency for which we have plotted results in Fig. 3. The probable error in measured spectral reflectance is less than 0.001 except in the vicinity of the resonance features,

where the probable error is 0.002.

Transmission Measurements

In measuring transmittance we employed techniques involving a wedge-shaped absorbing layer, which had been developed in our earlier work on water transmittance.⁶ A concave mirror produced an intermediate image of a Nernst glower inside the thin absorption cell; flux transmitted by the cell reached a second concave mirror which produced a final image of the glower at the entrance slit of a Perkin-Elmer Model 112 spectrometer. By moving the wedge cell laterally through the beam we could vary the thickness of the absorbing layer without altering reflection at the cell surfaces. The Lambert absorption coefficient α can be obtained from the ratio $I/I_1 = \exp[-\alpha(Z-Z_1)]$, where I and I_1 represent flux transmitted by film thicknesses Z and Z_1 , respectively. The cell windows used in the present work were polished rectangular CaF_2 crystals supplied by Harshaw Chemical Company; the windows were 38.5 mm long, 19.5 mm wide, and 5 mm thick. The windows were in close optical contact at one end and were separated by a 25- μm aluminum spacer at the other end.

The wedge cell C was mounted in a vacuum jacket as shown in Fig. 4. The CaF_2 windows were sealed to the cell's aluminum end plates with General Electric RTV-108 silicone adhesive. These end plates were sealed to the body of the cell by TEC low-temperature ring seals; similar ring seals connected the assembled cell to the stainless-steel reservoir R, which was filled with liquid ammonia. The upper end of the reservoir was attached by neoprene O-rings to the heavy external body E of the vacuum chamber, the end plates of which were equipped with CaF_2 windows W sufficiently large to

transmit the beam of radiant flux required to fill the optics of the spectrometer.

In order to minimize thermal shock to the cell windows we pre-cooled the cell by filling the reservoir with liquid ammonia when the orifice between the reservoir and the cell was closed by teflon plug P. The filled reservoir was allowed to stand for thirty minutes in order to bring the cell slowly into thermal equilibrium with the liquid ammonia at its equilibrium boiling point of -33.6° C. As in our earlier work we measured the thickness profile of the absorption cell interferometrically; we made a thickness-profile measurement prior to each set of transmission measurements with the cell pre-cooled but unfilled.

When the teflon plug had been removed, the pre-cooled cell filled rapidly; provided the cell windows were clean, the absorbing layer was free of bubbles. Admission of atmospheric water vapor to the reservoir was inhibited by means of a stopper in the top of the reservoir; ammonia vapor emerging from a small hole in the stopper was removed from the laboratory by an exhaust fan. Provided the liquid-ammonia level in the reservoir was several centimeters above the orifice to the cell, there was no evidence of water-vapor contamination.

The whole assembly shown in Fig. 4 was suspended from a cart which moved on tracks parallel to the cell windows. The cart, driven by a synchronous motor, moved the cell 30 mm laterally in 12 minutes; this time provided a complete lateral scan of the absorbing layer and was long compared with the one-second time constant employed in the amplifier-recorder system. With the spectrometer set for a given frequency ν , we obtained recorder traces

giving measures of transmitted flux as a function of absorbing film thickness Z ; from these traces we determined the Lambert absorption coefficient $\alpha(\nu)$.

In spectral regions of weak absorption, where $\alpha(\nu) < 100 \text{ cm}^{-1}$, it was necessary to use thicker absorbing layers to determine $\alpha(\nu)$. In such regions cells of uniform thickness can be employed; we used cells of thickness 16, 135, 300, and 855 μm . The thickness of the thinnest of these cells was measured interferometrically; the thicker cells were assembled with carefully measured lead spacers.

Figure 5 gives a plot of the measured values of the Lambert absorption coefficients; the curves represent the smoothed results of 3 to 10 independent measurements taken at each of 215 frequencies. The probable error in the values of $\alpha(\nu)$ given in the figure is less than 5 percent except at the peaks of the sharp absorption bands near 3300 cm^{-1} , where the probable error is 10 percent. In addition to the strong bands near 3300, 1630, and 1058 cm^{-1} , several minor absorption bands are visible in the upper panel of Fig. 5; these minor bands can be more clearly seen in the lower panel of the figure in which the ordinate scale has been expanded by a factor of 10.

Optical Constants

The imaginary part of the refractive index at frequency ν can be expressed as $n_i = \alpha/4\pi\nu = \lambda\alpha/4\pi$, where α is the Lambert coefficient. If n_i is known, the real part of the refractive index can be determined from the reflectance R at near-normal incidence from the Fresnel relation

$$n_r = \{(1 + R) + [(1 + R)^2 - (1 - R)^2(n_i^2 + 1)]^{1/2}\}/(1 - R) . \quad (1)$$

On the basis of our measurements of $\alpha(\nu)$ and $R(\nu)$, we have determined $n_r(\nu)$ and $n_i(\nu)$ in the range 5000 - 875 cm^{-1} .

We also used the Kramers-Kronig relation for phase-shift dispersion analysis of reflectance data to obtain n_r and n_i from our reflectance data. This relation states that, if the modulus $\rho(\nu) = [R(\nu)]^{1/2}$ of the complex reflectivity $\rho(\nu)e^{i\phi(\nu)}$ is known for all frequencies, then

$$\phi(\nu_0) = \frac{2\nu_0}{\pi} \int_0^{\infty} \frac{\ln \rho(\nu)}{\nu_0^2 - \nu^2} d\nu. \quad (2)$$

Although the value $\phi(\nu_0)$ is most strongly influenced by values of $\rho(\nu)$ in the immediate vicinity of ν_0 , values of $\rho(\nu)$ for all frequencies must be known if the K-K relation (2) is to be applied with rigor. Since our reflectance measurements were limited to the range 5100 to 350 cm^{-1} , we made assumptions regarding values outside this range. We assumed that the gentle slope of the $R(\nu)$ -vs- ν curve in Fig. 3 was maintained from 5100 to 10,000 cm^{-1} and that $R(\nu)$ was constant for $\nu > 10,000 \text{ cm}^{-1}$. For $\nu < 350 \text{ cm}^{-1}$, we assumed that $R(\nu)$ first decreased from its maximum value of 0.047 at 350 cm^{-1} to a minimum of 0.029 at 110 cm^{-1} and then rose to a value of 0.10 near 10 cm^{-1} . Provided the assumed curve is smooth and is smoothly connected to the measured reflectance curve, the exact shape seems to have little influence on the values of the optical constants

$$n_r = (1-R)/(1+R-2R^{1/2}\cos\phi) \quad (3)$$

$$n_i = (-2R \sin\phi)/(1+R-2R^{1/2}\cos\phi) \quad (4)$$

in the 5000-350 cm^{-1} range. In making the K-K analysis we used a computer program developed by Querry and his associates.⁷

The values of $n_r(\nu)$ obtained by the two methods are in remarkably good

agreement over the range 5000 to 875 cm^{-1} . The only serious disagreement is in the vicinity of the minimum near 1100 cm^{-1} , where the value of n_r obtained from Eq. (2) is slightly less than unity and the value given by the K-K analysis is 1.14. Figure 6 gives a plot of $n_r(\nu)$ -vs- ν ; values of $n_r(\nu)$ given by the K-K analysis are given by the dotted curve in the vicinity of 1100 cm^{-1} . All values of $n_r(\nu)$ for $\nu < 900 \text{ cm}^{-1}$ are supported only by K-K analysis. Linear extrapolation of the curve toward higher frequencies leads to the value 1.335 ± 0.005 obtained by Marcoux for the sodium D lines.¹ Table I lists values of $n_r(\nu)$ at closely spaced frequencies; the curve in Fig. 6 can be used in making interpolations. The uncertainty in tabulated values of n_r is estimated as ± 2 percent except in the vicinity of 1100 cm^{-1} .

Our best values of $n_i(\nu)$ are plotted in Fig. 7 and listed in Table I. Throughout the range from 7000 cm^{-1} to the CaF_2 cut off at 980 cm^{-1} values of n_i based on the Lambert coefficient are given; as noted earlier, the uncertainties involved are ± 5 percent except at the band peaks near 3300 cm^{-1} , where the uncertainty is ± 10 percent. The K-K values of $n_i(\nu)$ at the absorption maxima at 3300 and 1630 cm^{-1} are consistently lower than those based on transmission measurements, but agreement between the two sets of values improves at lower frequencies. In spectral regions between the strong bands, the K-K analysis gives small negative values of $n_i(\nu)$; in view of the large uncertainties in $R(\nu)$, these non-physical results are not altogether surprising. The values of $n_i(\nu)$ given in Table I and Fig. 7 for $\nu < 980 \text{ cm}^{-1}$ are based on the K-K analysis and have an estimated uncertainty of ± 15 percent.

Discussion of Results

The frequencies and shapes of the absorption bands as determined in the present work are in essential agreement with the results of earlier studies^{2,3} of liquid ammonia at ambient laboratory temperature and high pressure. By comparing the spectra of normal and deuterated ammonia with the vapor spectrum, earlier investigators have identified the band at 3366 cm^{-1} as the ν_3 fundamental and 3262 cm^{-1} band as the overtone $2\nu_4$; the ν_1 fundamental lies between the two but cannot be resolved in the spectrum of the liquid. The ν_2 fundamental appears at 1058 cm^{-1} and the ν_4 fundamental appears at 1631 cm^{-1} in the liquid. The weaker bands that we have observed for $\nu > 3400\text{ cm}^{-1}$ also appear close to the frequencies at which combination and overtone bands appear in the vapor spectrum.⁸

The strong band at 385 cm^{-1} and the weaker band at 785 cm^{-1} are in a spectral region not covered in earlier studies of liquid ammonia; the very weak band at 2286 cm^{-1} has been hitherto undetected. The bands at $\nu < 1000\text{ cm}^{-1}$ are tentatively attributed to intermolecular motions. It is possible that the weak band at 2286 cm^{-1} is a combination of ν_4 with one or more intermolecular modes of vibration. It is highly desirable that the spectral region $\nu < 1000\text{ cm}^{-1}$ be studied by transmission methods, since bands in this region have been detected only by the K-K analysis of our reflection data. Although no suitable window materials are available for quantitative studies of transmission in most of this region, polyethylene windows might be suitable for survey work. Quartz windows could be used for $\nu < 200\text{ cm}^{-1}$ in the far infrared.

The general agreement between our present results and those obtained in

the earlier transmission studies,^{2,3} which were conducted with the liquid ammonia in a closed system, gives added assurance that condensation of atmospheric water vapor did not lead to spurious results in the present study. Until more precise values of the optical constants become available, our values should prove useful in planetary studies. We are at present adapting our techniques to studies of solid ammonia, which is probably the major constituent in the cloud cover of the outer planets.

We offer our thanks to Professor Marvin R. Querry and his associates at the University of Missouri, Kansas City, for valuable assistance in the Kramers-Kronig analysis of the reflection data.

Legends for Figures

Fig. 1 The reflectometer used for near-normal incidence reflectance measurements. The final image I_3 was located at the entrance slit of a Perkin-Elmer Model 112 spectrometer equipped with a Reeder thermocouple; LiF, CaF_2 , NaCl, and CsBr prisms were used in appropriate spectral regions.

Fig. 2 The sample holder used for reflectance measurements. The liquid-ammonia sample S in a glass dish D and the reference mirror M were located at the bottom of a pair of connecting wells W of stainless steel, which were embedded in a block of polystyrene foam P; resistive heaters H below the mirror were used to inhibit condensation on the mirror surface.

Fig. 3 Spectral reflectance $R(\nu)$ of liquid ammonia at near-normal incidence.

Fig. 4 The wedge cell used for measurements of the transmission spectrum of liquid ammonia. The cell C was mounted below reservoir R; during pre-cooling procedures the orifice between R and C was closed by teflon plug P. The end plates of the vacuum jacket E were equipped with CaF_2 windows W.

Fig. 5 The Lambert absorption coefficient of liquid ammonia in cm^{-1} .

Fig. 6 The real part n_r of the refractive index of liquid ammonia.

Fig. 7 The imaginary part n_i of the refractive index of liquid ammonia. Values based on the Lambert coefficient are repeated in the lower panel, in which the ordinate has been expanded by a factor of 10.

Footnotes and References

*Supported in part by the National Aeronautics and Space Administration.

1. Jules E. Marcoux, *J. Op. Soc. Am.* 59, 998 (1969).
2. J. Corset, J. Guillermet, and J. Lascombe, *Bull. Soc. Chim. France* 5, 1231 (1966).
3. G. Seillier, M. Ceccaldi, J. P. Leickman, *Method. Phys. Anal.* 4, 388 (1968).
4. A. N. Rusk, D. Williams, and M. R. Querry, *J. Op. Soc. Am.* 61, 895 (1971).
5. John Strong, Procedures in Experimental Physics (Prentice Hall, Englewood Cliffs, New Jersey, 1938), p 376.
6. C. W. Robertson and D. Williams, *J. Op. Soc. Am.* 61, 1316 (1971).
7. G. M. Hale, M. R. Querry, A. N. Rusk, and D. Williams, *J. Op. Soc. Am.* (In Press)
8. G. Herzberg, Infrared and Raman Spectra of Polyatomic Molecules (D. Van Nostrand Company, Inc., Princeton, New Jersey, 1945), p 296.

TABLE I

OPTICAL CONSTANTS OF LIQUID AMMONIA IN THE INFRARED

ν in cm^{-1}	n_i	n_r	λ in μm
7000	1.5101		1.43
6900	1.5101		1.45
6800	1.5101		1.47
6700	1.5101		1.49
6600	1.5101		1.52
6500	1.5101		1.55
6500	1.5101		1.54
6450	1.5101		1.55
6400	1.5101		1.56
6350	1.5101		1.57
6300	1.5101		1.59
6200	1.5101		1.61
6100	1.5101		1.64
6000	1.5101		1.67
5900	1.5101		1.69
5800	1.5101		1.71
5700	1.5101		1.75
5600	1.5101		1.79
5500	1.5101		1.81
5400	1.5101		1.85
5300	1.5101		1.89
5200	1.5101		1.91
5200	1.5101		1.92
5180	1.5101		1.93
5160	1.5101		1.94
5140	1.5101		1.95
5100	1.5101	1.333	1.96
5080	1.5101	1.338	1.97
5060	1.5101	1.338	1.98
5040	1.5101	1.338	1.96
5020	1.5101	1.338	1.99
5000	1.5101	1.338	2.00
4980	1.5101	1.338	2.01
4960	1.5101	1.338	2.02
4960	1.5101	1.338	2.02
4930	1.5101	1.338	2.03
4910	1.5101	1.338	2.04
4850	1.5101	1.337	2.06
4800	1.5101	1.337	2.08
4700	1.5101	1.337	2.13
4650	1.5101	1.337	2.15
4600	1.5101	1.337	2.17
4500	1.5101	1.337	2.20
4560	1.5101	1.337	2.19
4540	1.5101	1.337	2.21
4520	1.5101	1.337	2.21
4500	1.5101	1.337	2.22

ν in cm^{-1}	n_i	n_r	λ in μm
4480	0.00037	1.0337	2.23
4460	0.00250	1.0337	2.24
4440	0.00156	1.0337	2.25
4420	0.00127	1.0337	2.26
4400	0.00110	1.0337	2.27
4380	0.00105	1.0337	2.28
4360	0.00100	1.0337	2.29
4340	0.00100	1.0337	2.30
4320	0.00107	1.0337	2.31
4300	0.00114	1.0337	2.32
4280	0.00120	1.0337	2.33
4260	0.00127	1.0337	2.34
4240	0.00132	1.0337	2.347
4220	0.00139	1.0337	2.35
4200	0.00147	1.0336	2.355
4180	0.00154	1.0336	2.361
4160	0.00161	1.0335	2.365
4140	0.00169	1.0334	2.367
4120	0.00176	1.0332	2.371
4100	0.00184	1.0331	2.377
4080	0.00191	1.0329	2.380
4060	0.00198	1.0324	2.382
4040	0.00206	1.0319	2.385
4020	0.00213	1.0312	2.391
4000	0.00219	1.0310	2.397
3980	0.00227	1.0286	2.395
3960	0.00235	1.0275	2.393
3940	0.00242	1.0269	2.399
3920	0.00247	1.0262	2.401
3900	0.00253	1.0251	2.405
3880	0.00258	1.0243	2.405
3860	0.00263	1.0238	2.407
3840	0.00267	1.0236	2.409
3820	0.00271	1.0235	2.411
3800	0.00275	1.0233	2.413
3780	0.00278	1.0231	2.415
3760	0.00281	1.0229	2.416
3740	0.00284	1.0227	2.417
3720	0.00287	1.0225	2.417
3700	0.00290	1.0224	2.417
3680	0.00292	1.0223	2.417
3660	0.00294	1.0222	2.417
3640	0.00296	1.0221	2.417
3620	0.00298	1.0220	2.417
3600	0.00300	1.0219	2.417
3580	0.00302	1.0218	2.417
3560	0.00304	1.0217	2.417
3540	0.00306	1.0216	2.417
3520	0.00308	1.0215	2.417
3500	0.00310	1.0214	2.417
3480	0.00312	1.0213	2.417
3460	0.00314	1.0212	2.417
3440	0.00316	1.0211	2.417
3420	0.00318	1.0210	2.417
3400	0.00320	1.0209	2.417
3380	0.00322	1.0208	2.417
3360	0.00324	1.0207	2.417
3340	0.00326	1.0206	2.417
3320	0.00328	1.0205	2.417
3300	0.00330	1.0204	2.417
3280	0.00332	1.0203	2.417
3260	0.00334	1.0202	2.417
3240	0.00336	1.0201	2.417
3220	0.00338	1.0200	2.417
3200	0.00340	1.0199	2.417
3180	0.00342	1.0198	2.417
3160	0.00344	1.0197	2.417
3140	0.00346	1.0196	2.417
3120	0.00348	1.0195	2.417
3100	0.00350	1.0194	2.417
3080	0.00352	1.0193	2.417
3060	0.00354	1.0192	2.417
3040	0.00356	1.0191	2.417
3020	0.00358	1.0190	2.417
3000	0.00360	1.0189	2.417
2980	0.00362	1.0188	2.417
2960	0.00364	1.0187	2.417
2940	0.00366	1.0186	2.417
2920	0.00368	1.0185	2.417
2900	0.00370	1.0184	2.417
2880	0.00372	1.0183	2.417
2860	0.00374	1.0182	2.417
2840	0.00376	1.0181	2.417
2820	0.00378	1.0180	2.417
2800	0.00380	1.0179	2.417
2780	0.00382	1.0178	2.417
2760	0.00384	1.0177	2.417
2740	0.00386	1.0176	2.417
2720	0.00388	1.0175	2.417
2700	0.00390	1.0174	2.417
2680	0.00392	1.0173	2.417
2660	0.00394	1.0172	2.417
2640	0.00396	1.0171	2.417
2620	0.00398	1.0170	2.417
2600	0.00400	1.0169	2.417
2580	0.00402	1.0168	2.417
2560	0.00404	1.0167	2.417
2540	0.00406	1.0166	2.417
2520	0.00408	1.0165	2.417
2500	0.00410	1.0164	2.417
2480	0.00412	1.0163	2.417
2460	0.00414	1.0162	2.417
2440	0.00416	1.0161	2.417
2420	0.00418	1.0160	2.417
2400	0.00420	1.0159	2.417
2380	0.00422	1.0158	2.417
2360	0.00424	1.0157	2.417
2340	0.00426	1.0156	2.417
2320	0.00428	1.0155	2.417
2300	0.00430	1.0154	2.417
2280	0.00432	1.0153	2.417
2260	0.00434	1.0152	2.417
2240	0.00436	1.0151	2.417
2220	0.00438	1.0150	2.417
2200	0.00440	1.0149	2.417
2180	0.00442	1.0148	2.417
2160	0.00444	1.0147	2.417
2140	0.00446	1.0146	2.417
2120	0.00448	1.0145	2.417
2100	0.00450	1.0144	2.417
2080	0.00452	1.0143	2.417
2060	0.00454	1.0142	2.417
2040	0.00456	1.0141	2.417
2020	0.00458	1.0140	2.417
2000	0.00460	1.0139	2.417
1980	0.00462	1.0138	2.417
1960	0.00464	1.0137	2.417
1940	0.00466	1.0136	2.417
1920	0.00468	1.0135	2.417
1900	0.00470	1.0134	2.417
1880	0.00472	1.0133	2.417
1860	0.00474	1.0132	2.417
1840	0.00476	1.0131	2.417
1820	0.00478	1.0130	2.417
1800	0.00480	1.0129	2.417
1780	0.00482	1.0128	2.417
1760	0.00484	1.0127	2.417
1740	0.00486	1.0126	2.417
1720	0.00488	1.0125	2.417
1700	0.00490	1.0124	2.417
1680	0.00492	1.0123	2.417
1660	0.00494	1.0122	2.417
1640	0.00496	1.0121	2.417
1620	0.00498	1.0120	2.417
1600	0.00500	1.0119	2.417
1580	0.00502	1.0118	2.417
1560	0.00504	1.0117	2.417
1540	0.00506	1.0116	2.417
1520	0.00508	1.0115	2.417
1500	0.00510	1.0114	2.417
1480	0.00512	1.0113	2.417
1460	0.00514	1.0112	2.417
1440	0.00516	1.0111	2.417
1420	0.00518	1.0110	2.417
1400	0.00520	1.0109	2.417
1380	0.00522	1.0108	2.417
1360	0.00524	1.0107	2.417
1340	0.00526	1.0106	2.417
1320	0.00528	1.0105	2.417
1300	0.00530	1.0104	2.417
1280	0.00532	1.0103	2.417
1260	0.00534	1.0102	2.417
1240	0.00536	1.0101	2.417
1220	0.00538	1.0100	2.417
1200	0.00540	1.0099	2.417
1180	0.00542	1.0098	2.417
1160	0.00544	1.0097	2.417
1140	0.00546	1.0096	2.417
1120	0.00548	1.0095	2.417
1100	0.00550	1.0094	2.417
1080	0.00552	1.0093	2.417
1060	0.00554	1.0092	2.417
1040	0.00556	1.0091	2.417
1020	0.00558	1.0090	2.417
1000	0.00560	1.0089	2.417
980	0.00562	1.0088	2.417
960	0.00564	1.0087	2.417
940	0.00566	1.0086	2.417
920	0.00568	1.0085	2.417
900	0.00570	1.0084	2.417
880	0.00572	1.0083	2.417
860	0.00574	1.0082	2.417
840	0.00576	1.0081	2.417
820	0.00578	1.0080	2.417
800	0.00580	1.0079	2.417
780	0.00582	1.0078	2.417
760	0.00584	1.0077	2.417
740	0.00586	1.0076	2.417
720	0.00588	1.0075	2.417
700	0.00590	1.0074	2.417
680	0.00592	1.0073	2.417
660	0.00594	1.0072	2.417
640	0.00596	1.0071	2.417
620	0.00598	1.0070	2.417
600	0.00600	1.0069	2.417
580	0.00602	1.0068	2.417
560	0.00604	1.0067	2.417
540	0.00606	1.0066	2.417
520	0.00608	1.0065	2.417
500	0.00610	1.0064	2.417
480	0.00612	1.0063	2.417
460	0.00614	1.0062	2.417
440	0.00616	1.0061	2.417
420	0.00618	1.0060	2.417
400	0.00620	1.0059	2.417
380	0.00622	1.0058	2.417
360	0.00624	1.0057	2.417
340	0.00626	1.0056	2.417
320	0.00628	1.0055	2.417
300	0.00630	1.0054	2.417
280	0.00632	1.0053	2.417
260	0.00634	1.0052	2.417
240	0.00636	1.0051	2.417
220	0.00638	1.0050	2.417
200	0.00640	1.0049	2.417
180	0.00642	1.0048	2.417
160	0.00644	1.0047	2.417
140	0.00646	1.0046	2.417
120	0.00648	1.0045	2.417
100	0.00650	1.0044	2.417
80	0.00652	1.0043	2.417
60	0.00654	1.0042	2.417
40	0.00656	1.0041	2.417
20	0.00658	1.0040	2.417
0	0.00660	1.0039	2.417

ν in cm^{-1}	n_i	n_r	λ in μm
2280	0.00130	1.0324	4.339
2260	0.00117	1.0313	4.342
2240	0.00114	1.0303	4.346
2220	0.00110	1.0322	4.351
2200	0.00116	1.0322	4.355
2150	0.00134	1.0311	4.365
2100	0.00161	1.0320	4.376
2050	0.00191	1.0318	4.388
2000	0.00221	1.0317	4.399
1950	0.00260	1.0315	4.413
1900	0.00336	1.0312	4.426
1850	0.00430	1.0310	4.441
1800	0.00524	1.0304	4.456
1750	0.00878	1.0296	4.471
1700	0.0129	1.0277	4.486
1650	0.018	1.0267	4.499
1600	0.029	1.0264	4.512
1550	0.0610	1.0266	4.519
1500	0.0584	1.0279	4.517
1450	0.0310	1.0298	4.525
1400	0.0211	1.0316	4.545
1350	0.0178	1.0318	4.567
1300	0.017	1.0315	4.590
1250	0.017	1.0309	4.614
1200	0.0177	1.0291	4.639
1150	0.0190	1.0277	4.660
1100	0.0246	1.0256	4.685
1050	0.0531	1.0213	4.709
1000	0.0204	1.0410	4.719
950	0.0369	1.0359	4.726
900	0.0306	1.0316	4.743
850	0.0272	1.0374	4.762
800	0.0205	1.0400	4.780
750	0.0130	1.0400	4.789
700	0.0250	1.0425	4.755
650	0.0119	1.0365	4.721
600	0.0087	1.0344	4.676
550	0.0132	1.0357	4.651
500	0.0116	1.0315	4.633
450	0.0065	1.0326	4.629
400	0.0023	1.0311	4.638
350	0.0061	1.0276	4.667
300	0.0034	1.0241	4.619
250	0.0019	1.0211	4.600
200	0.0018	1.0207	4.622
150	0.00236	1.0348	4.500
100	0.0021	1.0404	4.557

Fig. 1

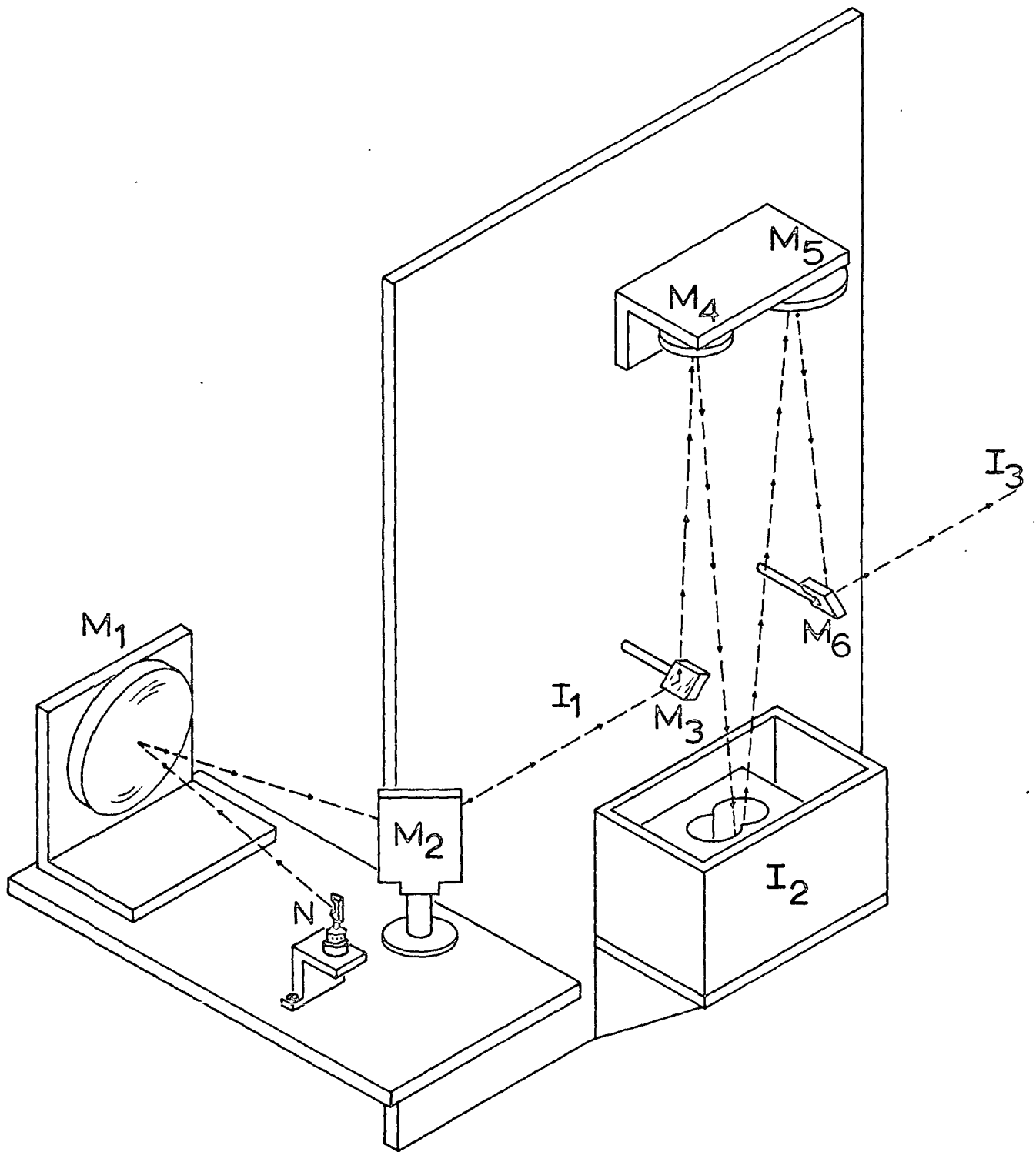
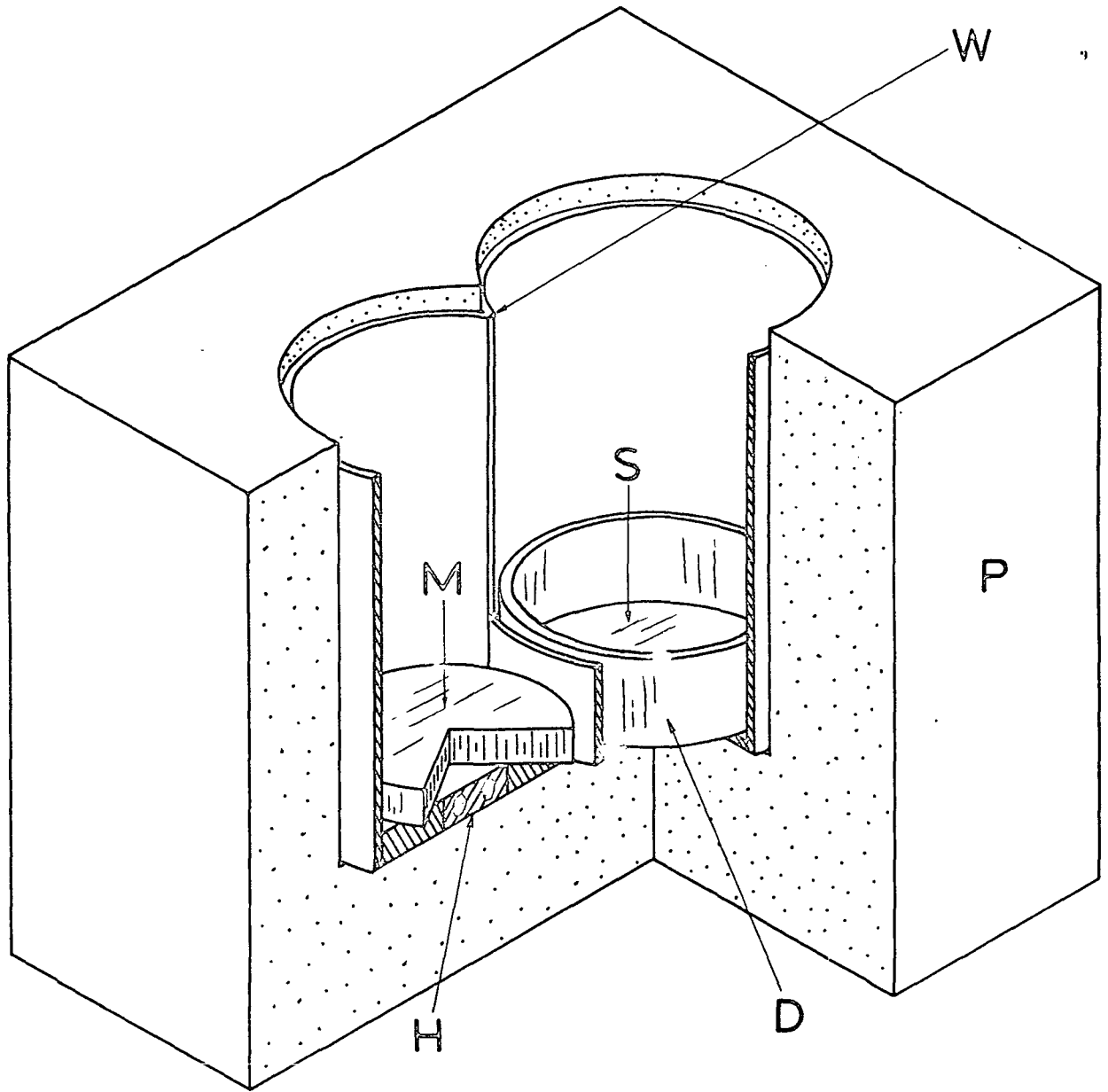


Fig. 2



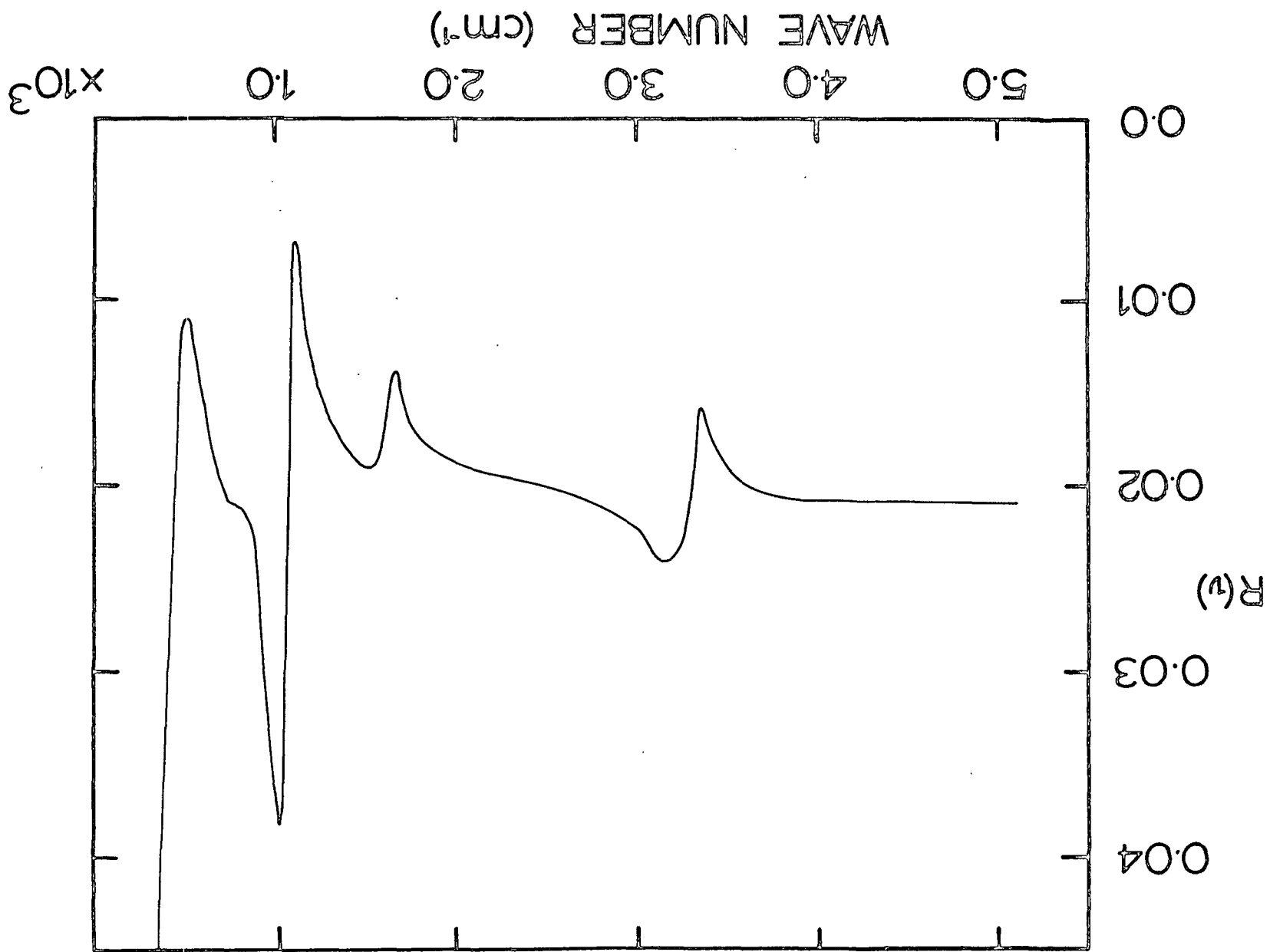
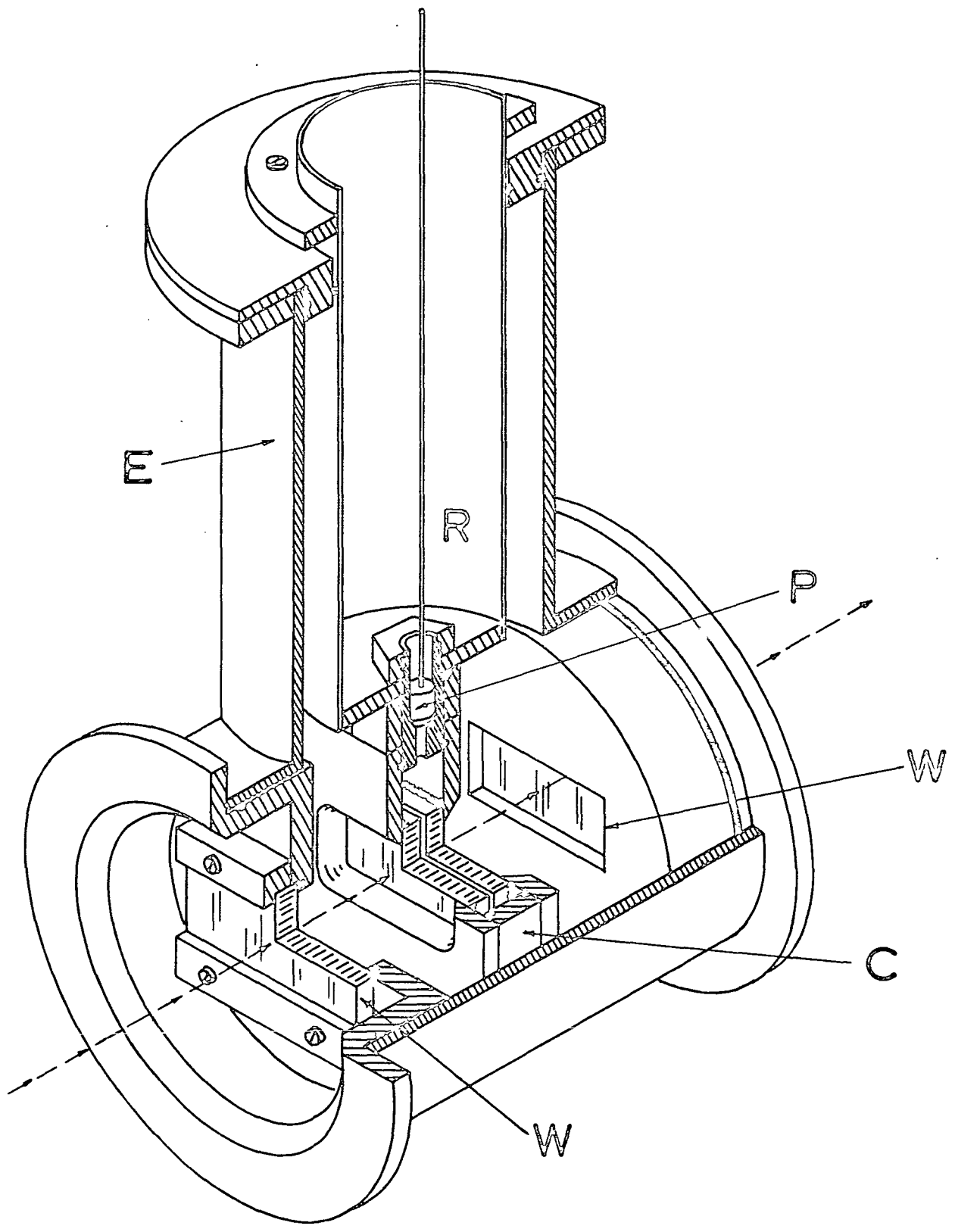


Fig. 3

Fig 4



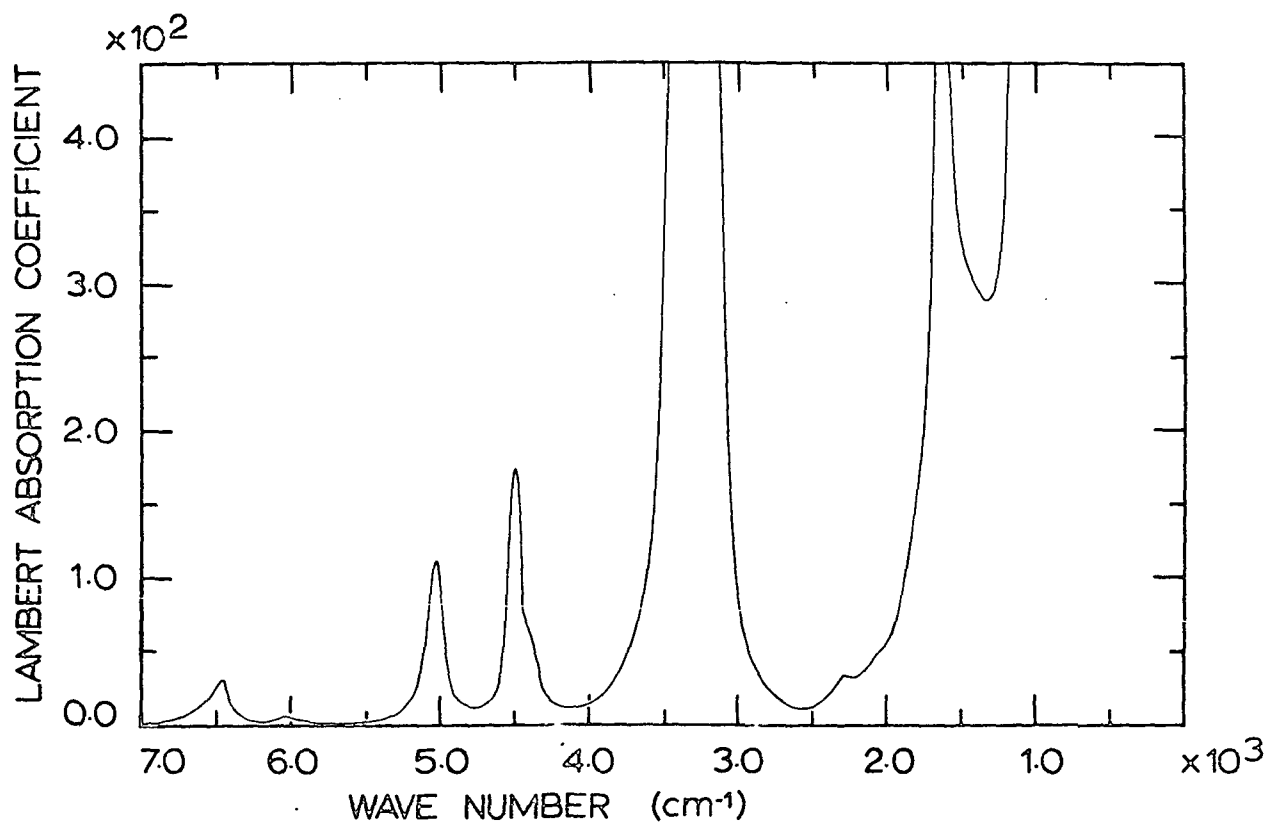
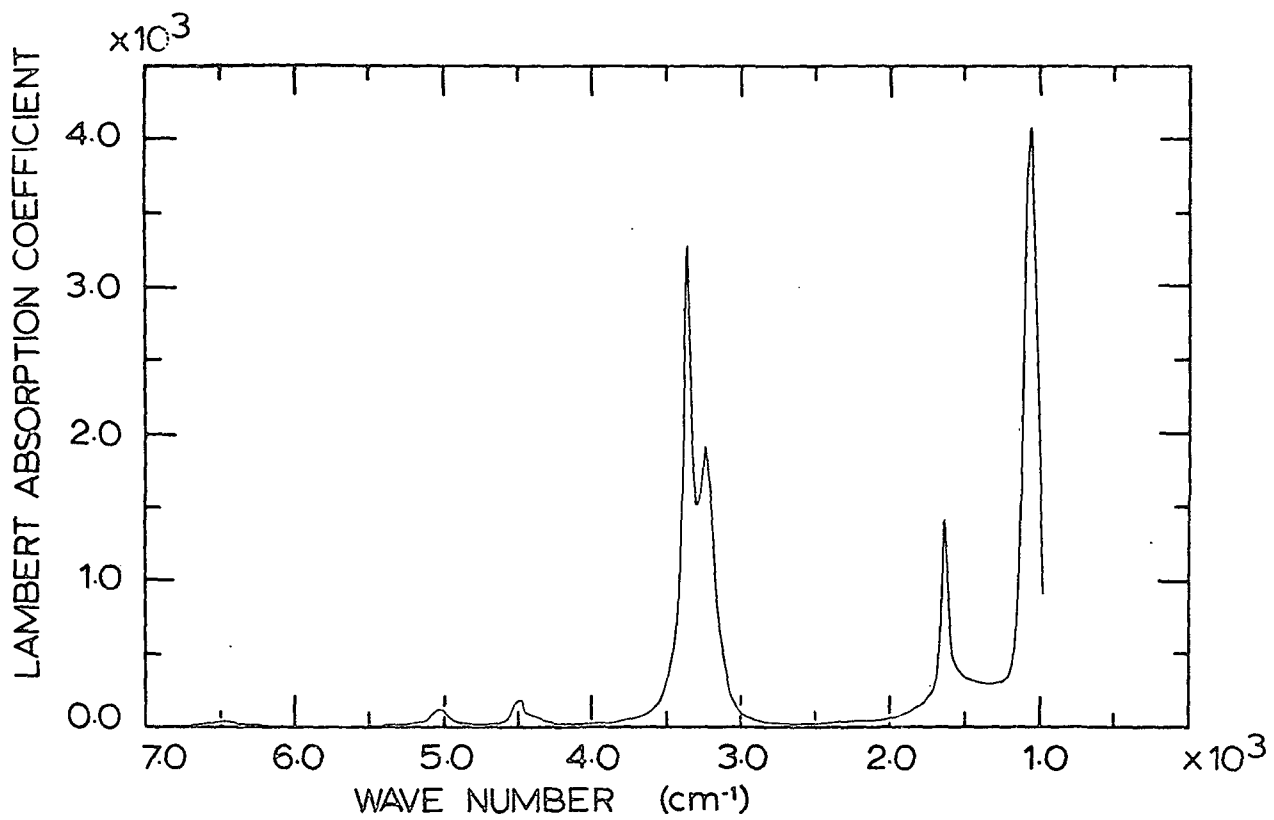


Fig. 5

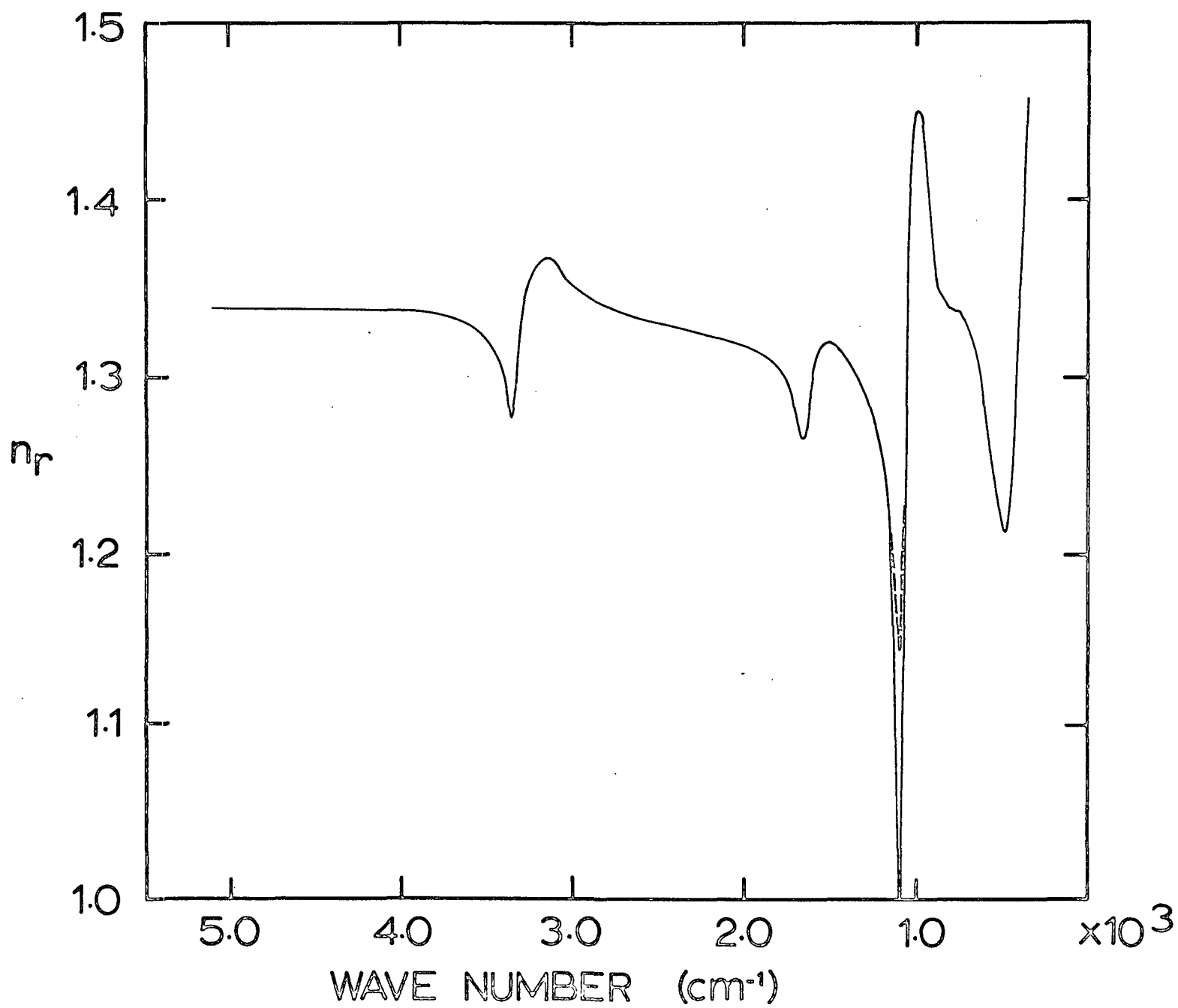


Fig. 6

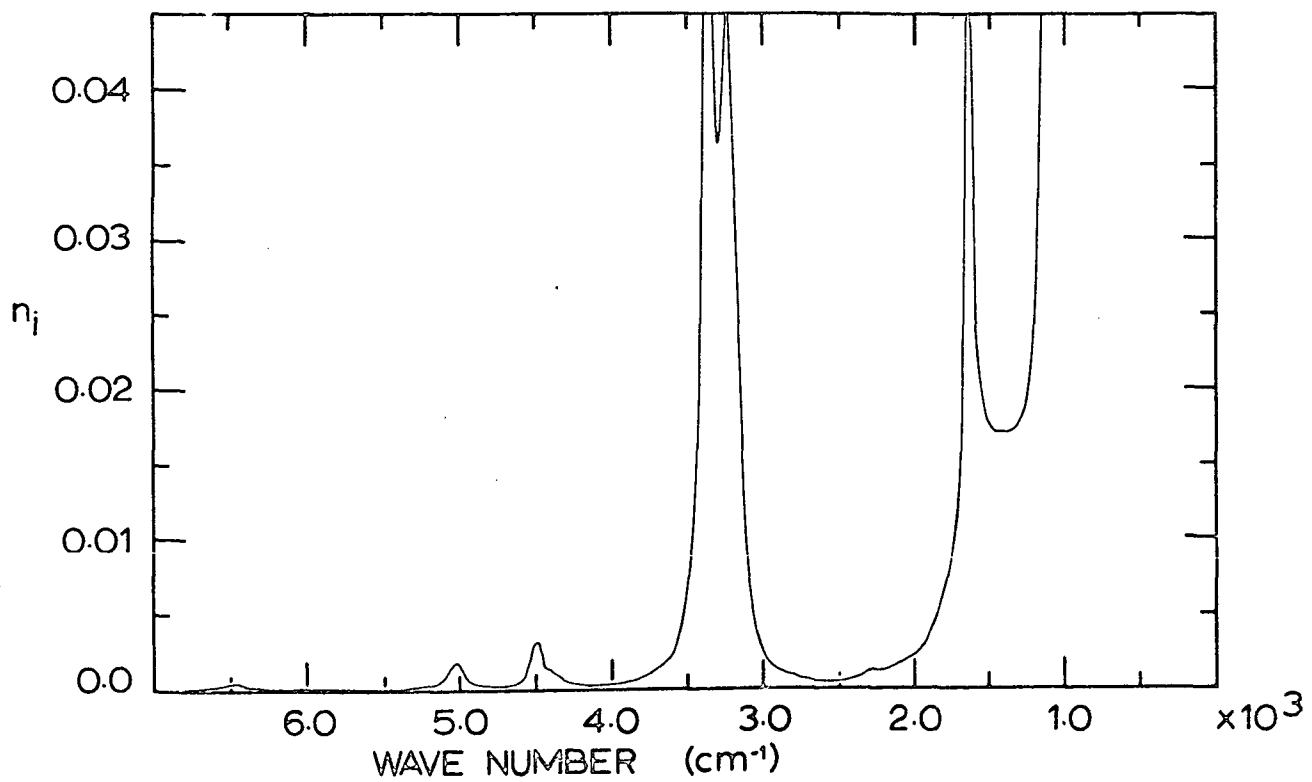
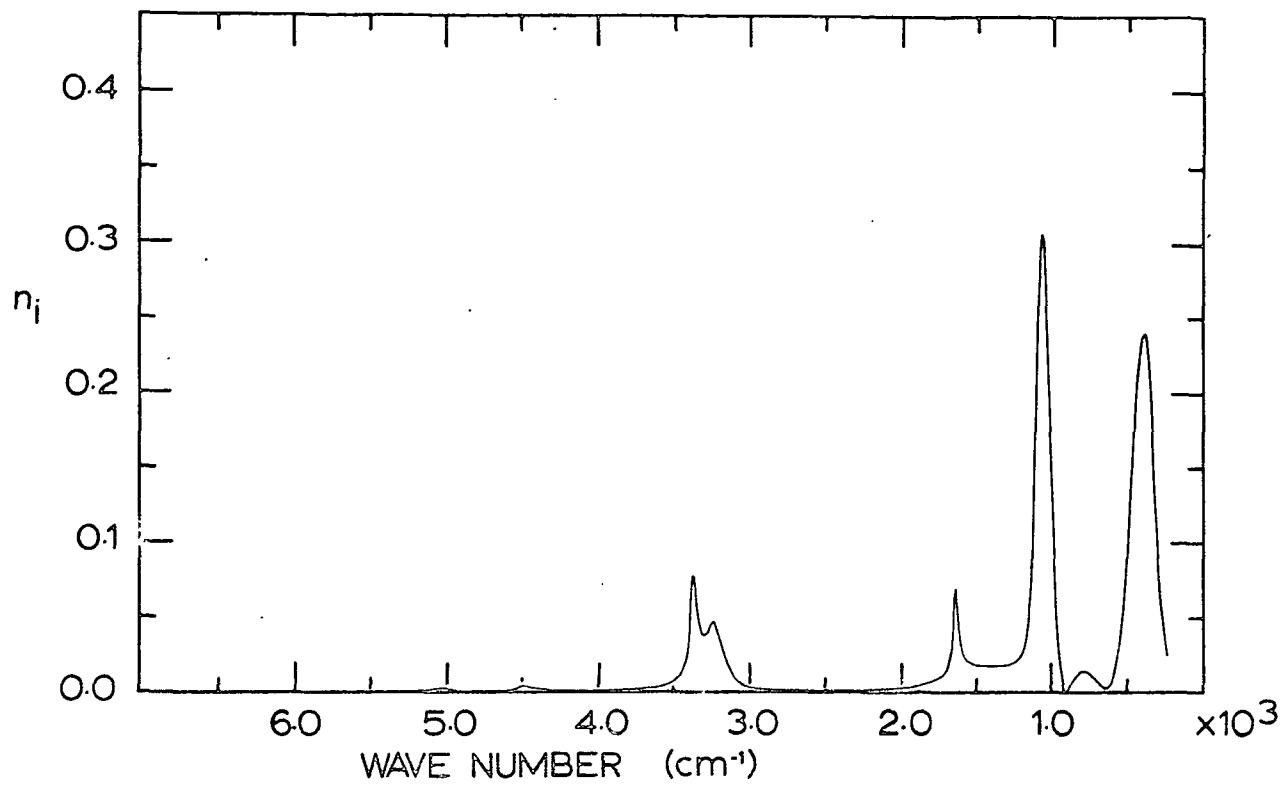


Fig. 7